Sharp habitat shifts, evolutionary tipping points and rescue: quantifying the perilous path of a specialist species toward a refugium in a changing environment

Léonard Dekens

Theoretical Population Biology 160 (2024) 25–48

Contents lists available at ScienceDirect

Theoretical Population Biology

journal homepage: www.elsevier.com/locate/tpb

Sharp habitat shifts, evolutionary tipping points and rescue: Quantifying the perilous path of a specialist species towards a refugium in a changing environment

Léonard Dekens

Theoretical Biology Lab, The Francis Crick Institute, London NW1 1AT, United Kingdom

ARTICLE INFO

Dataset link: https://github.com/ldekens/two-patch-model-changing-environment

Keywords:
Adaptation to a changing environment
Patchy environment
Quantitative genetic model
Habitat shift
Evolutionary tipping points

ABSTRACT

Specialist species thriving under specific environmental conditions in narrow geographic ranges are widely recognized as heavily threatened by climate deregulation. Many might rely on both their potential to adapt and to disperse towards a refugium to avoid extinction. It is thus crucial to understand the influence of environmental conditions on the unfolding process of adaptation. Here, I study the eco-evolutionary dynamics of a sexually reproducing specialist species in a two-patch quantitative genetic model with moving optima. Thanks to a separation of ecological and evolutionary time scales and the phase-line study of the selection gradient, I derive the critical environmental speed for persistence, which reflects how the existence of a refugium impacts extinction patterns and how it relates to the cost of dispersal. Moreover, the analysis provides key insights about the dynamics that arise on the path towards this refugium. I show that after an initial increase of population size, there exists a critical environmental speed above which the species crosses a tipping point, resulting into an abrupt habitat switch. In addition, when selection for local adaptation is strong, this habitat switch passes through an evolutionary "death valley", leading to a phenomenon related to evolutionary rescue, which can promote extinction for lower environmental speeds than the critical one.

1. Introduction

Biological context. Historical data highlights how climate change shifts the spatial distributions of species across taxa, especially polewards (Parmesan et al., 1999 on butterflies) or upwards in elevation (Lenoir et al., 2008 on plants, Moritz et al., 2008 on mammals). Predicting the interplay between changes in species distribution and species abundance and persistence is a crucial ongoing challenge (Ehrlén and Morris, 2015). It requires in particular a better understanding of the evolutionary strategies of adaptation in the face of climate change (Hoffmann and Sgrò, 2011). Among all species, specialist species have been found to be particularly vulnerable to the changing climate (Clavel et al., 2011). Since they are adapted to a limited niche width, opportunities to disperse and adapt to a potentially more suitable habitat are sparser, especially in increasingly fragmented environments (Berg et al., 2010, Adams-Hosking et al., 2012, Hof et al., 2012, Damschen et al., 2012). This issue highlights the importance of habitats that can act as refugia, which have already been shown to have played a major part in specialists' persistence in the past (Corlett and Tomlinson, 2020). Such refugia are recognized as key components in conservation efforts (Morelli et al., 2016). They can be thermal shelters located polewards to escape the rising temperatures, hydrological refugia in island-continent systems (McLaughlin et al., 2017, Ramirez et al., 2020) or edaphic refugia for soil specialists (Corlett and Tomlinson, 2020). These examples emphasize the relevance of incorporating a patchy spatial structure in models of adaptation to climate change to better understand the population dynamics of specialists species towards refugia in highly fragmented environments (Urban et al., 2016).

Theoretical models of adaptation to a changing environment in a single habitat: lag-load. To understand and predict how species adapt to a changing environment, one can turn to theoretical models. The case of gradually changing environments has been attracting sustained interest from modellers and theoreticians in quantitative genetics for over thirty years (see a review in Kopp and Matuszewski, 2014). One of the first lines of research focused on the demographic and trait dynamics of a panmictic population living in a single habitat, subjected to stabilizing selection around an optimal trait moving at a constant speed (Lynch and Lande, 1993; Bürger and Lynch, 1995; Lande and Shannon, 1996). The analysis highlights how maladaptation to the changing environment induces a lag between the population' mean trait and the optimal trait, which eventually stabilizes. This evolutionary load impacts the demography by decreasing the population size. In this case, these

E-mail addresses: leonard.dekens@gmail.com, leonard.dekens@crick.ac.uk.

https://doi.org/10.1016/j.tpb.2024.09.001
Received 18 October 2023
Available online 9 October 2024

studies derive a simple expression of the critical rate of environmental change above which the environment changes too fast for the population to persist and leads to extinction. The analytical results of these studies depend on the following assumptions: a Gaussian approximation of the trait distribution within the population and a quadratic selection function implying that fitness decreases more steeply away from the optimal trait. This approach has been extended to include the effects of plasticity (Chevin et al., 2010), multidimensional quantitative traits (Duputié et al., 2012), age-structure (Cotto and Ronce, 2014; Cotto et al., 2019) and the influence of the mode of reproduction (Bürger, 1999, Waxman and Peck, 1999, Bürger, 2000, Garnier et al., 2023).

Evolutionary tipping points. A more recent study (Osmond and Klausmeier, 2017) showed that the result of constant lag at equilibrium between the mean trait and the optimal trait is a consequence of the particular quadratic shape of the stabilizing selection function chosen in the references above. With this type of selection function, the selection gradient increases linearly with the distance between the population's mean trait and the moving optimum. For selection functions where the strength of selection instead fades away from the moving optimum, Osmond and Klausmeier (2017) showed that there exist evolutionary tipping points that abruptly lead the population to extinction upon a slight increase in the speed of environmental change. This happens because the lag between the mean trait and the optimal trait grows indefinitely past a certain threshold due to a change of convexity in the considered selection gradient. This feature (among others) was also characterized analytically in Garnier et al. (2023) who investigated more broadly the influence of the selection functions on the adaptation of sexually and asexually reproducing populations to a changing environment. However, while these evolutionary tipping points are linked to particular choices of selection functions in a single habitat framework, they have also been reported to arise in more complex frameworks (Klausmeier et al., 2020). For example, including an age structure in the population (Cotto and Ronce, 2014, Cotto et al., 2019) allows for feedback loops between the dynamics of the demography and of traits to create multiple co-existing equilibria that promote evolutionary tipping points. This last feature has also been related to tipping points in a broader variety of eco-evolutionary models (see Dakos et al., 2019): for example, abrupt switching between different developmental strategies in an oscillatory environment (Botero et al., 2015) or between ecosystem structure in shallow lake environments (Chaparro-Pedraza, 2021).

Spatial structure with a changing environment. As spatial structure provides species with the possibility to disperse when facing a changing environment, several theoretical quantitative genetic studies have included a spatial component in their models. A particularly rich line of research considers a species evolving in a continuous space, extending the concept of a gradually moving optimum in a single habitat to an environmental gradient shifting gradually at a constant speed. Stemming from the framework introduced by Pease et al. (1989), more and more sophisticated models have analysed how populations can track the shifting environmental gradient with a constant spatial lag when the speed of the environment is below a critical threshold, thus escaping extinction by shifting their spatial range. Extensions of this work study the influence of density-dependence (Polechová et al., 2009), or a multidimensional adaptive trait (Duputié et al., 2012). More recently, a study modelling two dispersal modes differing in their mean dispersal distance (pollen and seed dispersal) showed that long range-dispersal can trigger an ecological niche shift in addition to the spatial range shift, which buffers the species for greater environmental speeds (Aguilée et al., 2016). All these analyses rely heavily on the analytical travelling waves toolkit that is specifically designed to study the long-term effect of dispersal in a continuous space (see Alfaro et al., 2017, Roques et al., 2020 and Lavigne, 2023 for precise mathematical treatments of the case of asexual populations).

However, these methods are not well suited to study the patterns of dispersal in fragmented and patchy environments, where the demographic dynamics and the trait dynamics are quite difficult to disentangle, even under a stable environment (see Ronce and Kirkpatrick, 2001; Hendry et al., 2001; Holt et al., 2003; Dekens, 2022 for sexual reproduction and Débarre et al., 2013; Mirrahimi, 2017; Mirrahimi and Gandon, 2020 for asexual ones). Therefore, most models studying adaptation to a changing and fragmented environment rely mostly on numerical simulations to explore complex metacommunity dynamics (see Cotto et al., 2017 for such a model with multiple traits, species and an age structure, and Walters and Berger, 2019 on the contribution of genetic variance on the time to extinction in a migration–mutation–selection–drift framework), or to assess the interplay between dispersal and local competition under a warming climate (Thompson and Fronhofer, 2019, McManus et al., 2021). Moreover, simulations of a quantitative genetic two-patch model suggest that a changing environment can first lead to sharp declines in subpopulation size with a potential rebound when it stabilizes, but less so for specialists (Bourne et al., 2014).

As it is important to quantify these sharp dynamics and predict the conditions under which they occur, I propose here to analyse a two-patch quantitative genetic model under a changing environment that considers a specialist species that is initially well adapted to its native habitat. This model aims at improving our understanding of the evolutionary mechanisms the specialist species undergoes to potentially leverage the existence of a refugium when the native habitat becomes nonviable. Indeed, under a changing environment, such a species is expected to lag behind the optimum of the native habitat, and thus to be closer to the refugium's one. Under which conditions do species keep pace with their native habitat? If the environmental speed is too great, will they be forced to adapt to the refugium, and if so, how successfully? To answer these questions, I will start by leveraging the results of an analogous model under stable environment (Dekens, 2022) that includes the analytical derivation of the source–sink dynamics characteristic of a specialist species.

Outline of the paper. In this work, I study the eco-evo dynamics of a sexual population in a fragmented and changing environment thanks to a two-patch quantitative genetic model with moving optima. More precisely, I consider a specialist population initially adapted to one of the two habitats (their native habitat), whose migrants fail to establish themselves in the other one at first (the refugium). My aim is to analytically predict the dynamics of niche evolution of this specialist population as a function of the speed of environmental change. To carry out this aim, in Section 2, I show that, in a regime of small within-family variance allowing a separation of ecological and evolutionary time scales, all features of the dynamics of adaptation can be deduced from a simple modification of the phase-line analysis of the selection gradient derived in a previous study of a two-patch model under stable environment (Dekens, 2022).

The results are presented in Section 3. Firstly, for low environmental speeds, the metapopulation actually increases in size, as it benefits from becoming less specialized to the native habitat. In addition, there exists an intermediate critical environmental speed leading to an abrupt habitat switch from the native habitat to the refugium. Such a switch corresponds to an evolutionary tipping point and is therefore difficult to reverse. Moreover, above a selection threshold leading to the creation of an evolutionary "death valley" between the habitats, the population can experience an evolutionary rescue during the habitat switch. Finally, I quantify the critical speed of environmental change above which the population becomes too maladapted and goes extinct in this native habitat/refugium framework. Contrary to the classical prediction in a single-habitat framework, I show that the critical speed does not always increase with selection strength and can be discontinuous.

2. Methods

2.1. Model

The model follows a classical framework of quantitative genetic models for heterogeneous environments with continuous time (Ronce and Kirkpatrick, 2001; Hendry et al., 2001; Débarre et al., 2013; Mirrahimi and Gandon, 2020; Dekens, 2022), which is illustrated in Fig. 1. It considers a sexually reproducing species that lives in a fragmented two-patch environment, where one patch represents the species' native habitat, to which it is initially specialized, and the other a refugium, to which the species is initially not adapted. These habitats are connected by backward and forward migration at a constant instantaneous rate $\boldsymbol{m} \in \mathbb{R}_+^*$, meaning that, during each infinitesimally small time interval $dt \ll 1$, an average proportion $\boldsymbol{m} \times dt$ of the population migrate from each habitat to the other. Moreover, individuals are characterized by the value of a quantitative trait $\boldsymbol{z} \in \mathbb{R}$, which quantifies their adaptation to their local habitat. In each habitat (indexed by i), the subpopulation is thus described by its temporal trait distribution $\boldsymbol{n_i}(t, z)$ (t is the time variable). Within each habitat i, individuals mate randomly at a constant rate $\boldsymbol{r} \in \mathbb{R}_+^*$ and die due to two biological processes. The first is density-dependent regulation at a rate $\boldsymbol{\kappa} \times \boldsymbol{N_i}(t) > 0$, where $\boldsymbol{N_i}(t) := \int_{\mathbb{R}} \boldsymbol{n_i}(t, z)dz$ is the local subpopulation size at time t and $\boldsymbol{\kappa} \in \mathbb{R}_+^*$ is a constant multiplicative parameter representing the pressure of competition for resources. The individuals also suffer from a lethal local stabilizing selection depending on the value of their quantitative trait $\boldsymbol{z} \in \mathbb{R}$. More precisely, death by stabilizing selection is minimalized at a local trait optimum ($\boldsymbol{\theta_2}(t)$ in the native habitat and $\boldsymbol{\theta_1}(t)$ in the refugium, with $\boldsymbol{\theta_1}(t) < \boldsymbol{\theta_2}(t)$) and decreases quadratically away from it according to the selection function $\boldsymbol{z} \mapsto -\boldsymbol{g} \times (\boldsymbol{z} - \boldsymbol{\theta_i}(t))^2$ (in habitat i). In the last expression, $\boldsymbol{g} \in \mathbb{R}_+^*$ is a constant parameter representing the strength of the local stabilizing selection (a larger $\boldsymbol{g}$ leads to a stronger death rate away from the local optimum, all else being held equal). The two local optima are assumed to shift at the same constant speed $\boldsymbol{c} > 0$, which models the action of the shifting environment: $\boldsymbol{\theta_i}(t) = (-1)^i\boldsymbol{\theta} + \boldsymbol{ct}$. Individuals are characterized by a quantitative trait whose value $\boldsymbol{z} \in \mathbb{R}$ determines their adaptation to the habitat they live in. This quantitative trait is thought to have a highly polygenic basis with small additive allelic effects, and its inheritance across generations is modelled by the infinitesimal model (Fisher, 1919; Bulmer, 1971; Turelli and Barton, 1990; Barton et al., 2017). The infinitesimal model in its additive version states that the distribution of the trait within each family is Gaussian, centred on the mean parental trait and with variance $\boldsymbol{\sigma}^2$, which reads

$$(\boldsymbol{z_1}, \boldsymbol{z_2}) \mapsto \frac{\boldsymbol{z_1} + \boldsymbol{z_2}}{2} + \mathcal{N}_{0,\boldsymbol{\sigma}^2},$$

where $\boldsymbol{z_1}$ and $\boldsymbol{z_2}$ represent the two parental traits. The parameter $\boldsymbol{\sigma}^2$ is the within-family variance (also called segregational variance). In this model, it is assumed to be constant across families, time and space. Accordingly, at a time t, the number of individuals born with a trait of value $\boldsymbol{z}$ in the habitat i is given by the following formula (also used by Turelli and Barton, 1990; Mirrahimi and Raoul, 2013; Calvez et al., 2019; Patout, 2023; Dekens and Lavigne, 2021; Dekens, 2022; Garnier et al., 2023):

$$\boldsymbol{\mathcal{B}_\sigma}[\boldsymbol{n_i}](t, \boldsymbol{z}) = \iint_{\mathbb{R}^2} G_{0,\boldsymbol{\sigma}^2}\left(\boldsymbol{z} - \frac{\boldsymbol{z_1} + \boldsymbol{z_2}}{2}\right) \boldsymbol{n_i}(t, \boldsymbol{z_1}) \frac{\boldsymbol{n_i}(t, \boldsymbol{z_1})}{\boldsymbol{N_i}(t)} d\boldsymbol{z_1} d\boldsymbol{z_2}. \tag{1}$$

We consider the dynamics of the local trait distributions given by:

$$\begin{cases} \partial_t \boldsymbol{n_1}(t, \boldsymbol{z}) = \boldsymbol{r}\boldsymbol{\mathcal{B}_\sigma}[\boldsymbol{n_1}](t, \boldsymbol{z}) - \boldsymbol{g}(\boldsymbol{z} - \boldsymbol{\theta_1}(t))^2 \boldsymbol{n_1}(t, \boldsymbol{z}) - \boldsymbol{\kappa} \boldsymbol{N_1}(t) \boldsymbol{n_1}(t, \boldsymbol{z}) \\ \qquad\qquad + \boldsymbol{m}\left(\boldsymbol{n_2}(t, \boldsymbol{z}) - \boldsymbol{n_1}(t, \boldsymbol{z})\right), \\ \partial_t \boldsymbol{n_2}(t, \boldsymbol{z}) = \boldsymbol{r}\boldsymbol{\mathcal{B}_\sigma}[\boldsymbol{n_2}](t, \boldsymbol{z}) - \boldsymbol{g}(\boldsymbol{z} - \boldsymbol{\theta_2}(t))^2 \boldsymbol{n_2}(t, \boldsymbol{z}) - \boldsymbol{\kappa} \boldsymbol{N_2}(t) \boldsymbol{n_2}(t, \boldsymbol{z}) \\ \qquad\qquad + \boldsymbol{m}\left(\boldsymbol{n_1}(t, \boldsymbol{z}) - \boldsymbol{n_2}(t, \boldsymbol{z})\right). \end{cases} \tag{P}$$

2.2. Overview of the analysis

In this section, I explain how to conveniently transform the PDE system (*P*) in order to isolate the influence of the changing environment, which allows leveraging the main ideas of the analysis under stable environment done in Dekens (2022). Indeed, I show that, in a chosen regime of small within-family variance, the full dynamics of local trait distributions can be summarized by the dynamics of two time-dependent variables: the ratio of the two subpopulation sizes and the mean trait of the metapopulation. In addition, I show that in the final system (S_0), the environmental change directly influences only the dynamics of the latter, and only linearly. I refer the interested reader who wishes to learn about all the mathematical details underlying this section to Appendix A.

1. Small within-variance regime and moving-frame reference. I place the analysis in the regime where the within-family variance $\boldsymbol{\sigma}^2$ is small compared to the difference between the local optima ($\boldsymbol{\theta_2} - \boldsymbol{\theta_1} = 2\boldsymbol{\theta}$). This is likely to be the case after a long time at equilibrium under stabilizing selection and stable environment. I then introduce a small parameter $\varepsilon^2 := \frac{2\boldsymbol{\sigma}^2}{\boldsymbol{\theta}^2} \ll 1$ underlying this regime of small within-family variance. In this regime, the local genetic variances are expected to remain small (of order ε^2), so local mean traits take a long time to shift under the action of local selection (see Dekens (2022)). Therefore, it is practical to rescale the time to match the timescale of the evolution of the local mean traits. It is also convenient to place the analysis in the moving-frame reference whose speed matches the environmental speed and in which the local optimal traits are fixed. In the first paragraph of Appendix A, I detail how to rescale the variables and parameters of my model according to (7) in order to get the following dimensionless system (P_ε) from (*P*):

$$\begin{cases} \varepsilon^2 \partial_t n_{\varepsilon,1}(t, z) - \varepsilon^2 c \partial_z n_{\varepsilon,1}(t, z) = \mathcal{B}_\varepsilon[n_{\varepsilon,1}](t, z) - g(z+1)^2 n_{\varepsilon,1}(t, z) \\ \qquad\qquad - N_{\varepsilon,1}(t) n_{\varepsilon,1}(t, z) + m\left(n_{\varepsilon,2}(t, z) - n_{\varepsilon_1}(t, z)\right), \\ \varepsilon^2 \partial_t n_{\varepsilon,2}(t, z) - \varepsilon^2 c \partial_z n_{\varepsilon,2}(t, z) = \mathcal{B}_\varepsilon[n_{\varepsilon,2}](t, z) - g(z-1)^2 n_{\varepsilon,2}(t, z) \\ \qquad\qquad - N_{\varepsilon,2}(t) n_{\varepsilon,2}(t, z) + m\left(n_{\varepsilon,1}(t, z) - n_{\varepsilon,2}(t, z)\right). \end{cases} \tag{P_ε}$$

From now on, I will refer to these rescaled quantities, which will be not bolded.

2. Parameter range considered and initial specialized population. In all that follows, I examine the case where the parameter of the strength of selection g is large enough relative to the migration rate m such that specialist equilibria exist and are stable under a stable environment: $1 + 2m < 5g$ (see Proposition 4.2 of Dekens, 2022). With the original parameters, the last condition equates to $\boldsymbol{r} + 2\boldsymbol{m} < 5\boldsymbol{g}\boldsymbol{\theta}^2$. I also assume that this strength of selection parameter g is bounded by above when the migration rate m is strong ($m > 1$) such that the identified specialist equilibria are viable, which reads: $g(m-1) < m^2$ (see also Proposition 4.2 of Dekens, 2022). With the original parameters, the last condition equates to $\boldsymbol{g}\boldsymbol{\theta}^2(\boldsymbol{m} - \boldsymbol{r}) < \boldsymbol{m}^2$. Under these conditions, there exist two viable specialist equilibria according to mirrored source–sink dynamics (see also Ronce and Kirkpatrick, 2001; Holt et al., 2003). For the initial state of the system, I choose the equilibrium describing a species specialized in the native habitat whose precise characterization is indicated in the Proposition 4.2 of Dekens (2022).

3. Gaussian approximation of local trait distributions. In the chosen regime of small within-family variance $\varepsilon^2 \ll 1$, the arguments developed in Dekens (2022) ensure that the local trait distributions are approximately Gaussian, with a small variance ε^2 (twice the within-family variance). Therefore, the moment-based ODE system describing the dynamics of the subpopulations sizes and the local mean traits is closed (see (M_ε)). I choose to report the analysis on this moment-based ODE system instead of the full PDE system on the local trait

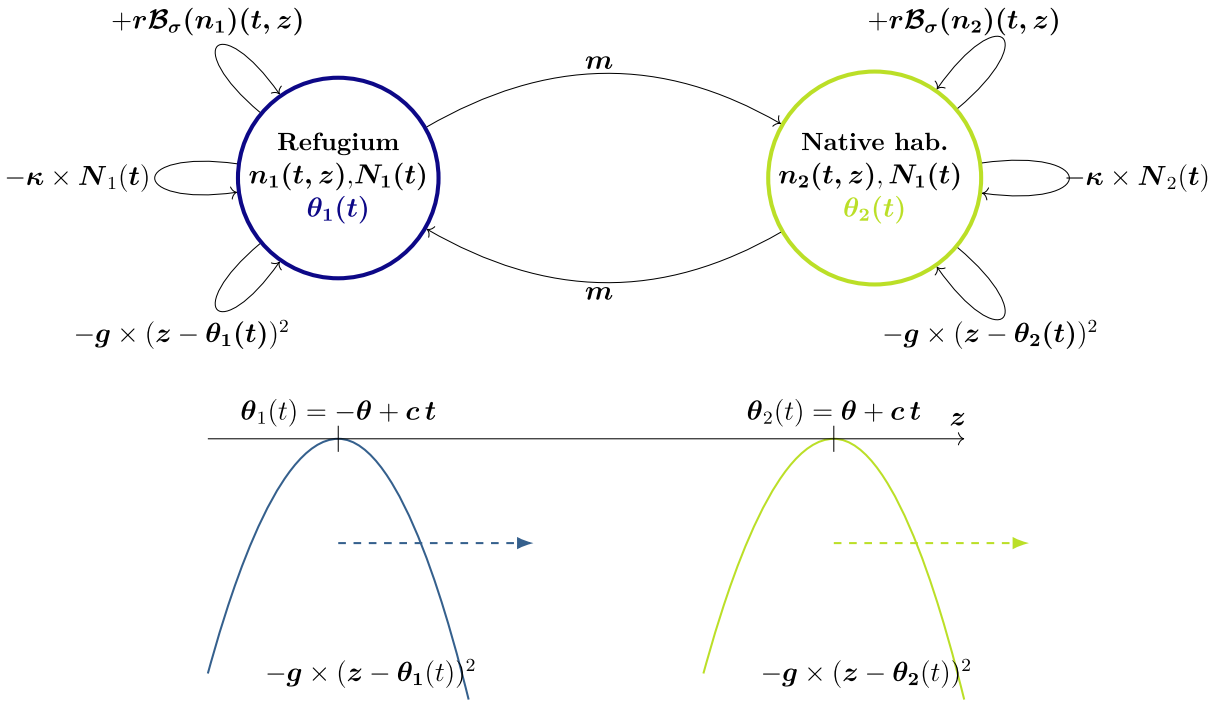

Fig. 1. Two-patch changing environment framework for a quantitative trait.

distributions (see the second paragraph of Appendix A for details about the derivation of such a moment-based system).

4. Separation of time scales and limit system. To disentangle the coupled dynamics of the subpopulations sizes and the local mean traits, one can leverage the fact that the local selection terms driving the dynamics of the mean traits are proportional to the small local genetic variances(see (M_ε)). This implies that the moment-based system (M_ε) can be reformulated as (S_ε) that highlights the interplay between fast and slow dynamics (see Appendix A). More precisely, there exists a separation of time scale between fast ecological phenomena (birth/death/migration) and slow evolutionary ones (shift of the local mean traits by selection), similarly to the analysis of Dekens (2022). In the third paragraph of Appendix A, I show that this leads to a limit system with greatly reduced complexity, as it only involves the ratio between subpopulations sizes $\rho(t) := \frac{N_2(t)}{N_1(t)}$ and the metapopulation's mean trait $Z(t)$ as variables. This limit system reads

$$\begin{cases} P_{Z(t)}(\rho(t)) = 0, \qquad \rho(t) > f_1(Z(t)), \\ \frac{dZ}{dt} = -c + 2g\left[\frac{\rho(t)-\frac{1}{\rho(t)}}{\rho(t)+\frac{1}{\rho(t)}} - Z(t)\right] \\ (Z(0),\rho(0)) = \left(Z^*_{\text{spec}}, \rho^*_{\text{spec}}\right). \end{cases} \tag{S_0}$$

In the next paragraphs, I describe and interpret biologically each component of (S_0).

The algebraic equality in the first line of (S_0) describes the fact that, in the considered slow timescale at any given time t, the system is at ecological equilibrium. This ecological equilibrium depends on the current metapopulation mean trait $Z(t)$. The ratio of subpopulation sizes $\rho(t)$ defining this ecological equilibrium is solution of the third-order polynomial

$$P_{Z(t)}(X) := X^3 - f_1(Z(t))X^2 + f_2(Z(t))X - 1,$$

where $f_1(Z) := 1+\frac{g}{m}(Z+1)^2-\frac{1}{m}$ and $f_2(Z) := 1+\frac{g}{m}(Z-1)^2-\frac{1}{m}$ (further details can be found in Lemma 1 of Dekens, 2022). The inequality of the first line in (S_0) represents the constraint that this ecological equilibrium must define a positive population size. This translates that the scope of the limit system (S_0) is restricted to describe the evolutionary dynamics of persisting populations (while indicating in contrast the range of parameters where the population is expected to go extinct). Importantly, non-trivial dynamics close to extinction are necessarily not well captured by this limit system. Additionally, one might notice that the first line is not directly impacted by the speed of environmental change c. This is because the ecological equilibrium revolves around the subpopulation sizes, which are not impacted directly by the changing environment, in line with Remark A.1 (see also the paragraph above (M_ε) in Appendix A).

The second line involves a differential equation describing the slow dynamics of the metapopulation mean trait Z. These dynamics are influenced by environmental change through the term $-c$ and by a combination of the two local stabilizing selections through the term $2g\left[\frac{\rho(t)-\frac{1}{\rho(t)}}{\rho(t)+\frac{1}{\rho(t)}} - Z(t)\right]$. More precisely, this last term can be interpreted as the selection gradient pushing with a strength g towards the following trait optimum $\tilde{\theta}(t) := \frac{\rho(t)-\frac{1}{\rho(t)}}{\rho(t)+\frac{1}{\rho(t)}}$. This composite optimum integrates the demographic feedback of the ecological dynamics on the evolutionary ones. Notice also that the trait variance of the metapopulation does not appear in this selection gradient. This is because, as mentioned after (8) in Appendix A, the slow timescale involved in the evolutionary dynamics of the metapopulation mean trait Z is precisely the one where the trait variance in the metapopulation scales to 1, so as to follow the action of selection on Z.

Finally, $\left(Z^*_{\text{spec}}, \rho^*_{\text{spec}}\right)$ are the initial values defined in Appendix A.

The keen reader might notice that (S_0) is almost the same as the analogous one derived in Dekens (2022) under stable environment. The only but crucial difference is that here, the changing environment pushes the metapopulation's mean trait $Z(t)$ backwards with a speed $-c$, which results in a lag (remember that the analysis is done in the moving-frame reference). Although this could look like a rather benign change, it leads to very rich dynamics that I detail in Section 3. In the next subsection, I explain how to use (S_0) in a simple way to predict these dynamics.

Remark 2.1 (*Analytical Relationship Between of* (P_ε) *and* (S_0) *and Their Biological Scope*)**.** I would like to stress the respective advantages and

drawbacks of the two settings underlying the analysis here. The first is represented by the PDE system (P_ε) that considers a small but positive within-family variance $\frac{\varepsilon^2}{2} > 0$. It is the most relevant biologically, as it corresponds to a clear biological and quantitative hypothesis about the within-family variance. In this parameter regime, I derive the closed ODE system (S_ε) from (P_ε). However, in both (P_ε) and (S_ε), the different dynamics at play (ecological and evolutionary) are too tangled for analysis to be tractable. That is why I further introduce the limit system (S_0). Its solutions are obtained by convergence of solutions of (S_ε) when ε vanishes, in the range of parameters where the solutions of (S_ε) describe a viable population. Its analytical complexity is sufficiently reduced so that the analysis can progress forward with the aim to get an approximation of the steady states of (P_ε). However, one needs to keep in mind that the limit case is of interest only as long as the solutions of (S_0) are a good approximation of the solutions of (P_ε) that are ultimately the most biologically meaningful. In particular, it is important to stress that the convergence of the solutions of (S_ε) towards the solutions of (S_0) is not necessarily ensured when they describe non-viable states of the population. Therefore, for such states, which will play an important role in some part of the subsequent analysis, the solutions of (P_ε) (or (S_ε)) can actually be quite different from the solutions of (S_0). This is why it is crucial to also rely on numerical resolutions of (P_ε) to get a complete depiction of the dynamics of the population for those cases in order to decipher whether the steady states derived from (S_0) are actually reached.

‘

2.3. Predicting the new equilibrium under a changing environment with a phase lines' study

Consider the first line of (S_0). For a given average trait in the metapopulation $Z(t)$, it states that $\rho(t)$ is a (positive) root of $P_{Z(t)}$. In the case where such a root is uniquely defined, $\rho(t)$ can be seen as a well-defined function of $Z(t)$. In this case, I use the notation $\rho(Z(t))$ (see Section 3 of Dekens, 2022 for the analytical conditions under which this happens). In this case, one can circumvent the first algebraic equation of (S_0) to reduce the analysis to the following autonomous differential equation only on Z (ie. the time variable is not directly involved):

$$\begin{cases} \frac{dZ}{dt} = -c + \mathcal{F}^{c=0}(Z), \qquad \rho(Z) > f_1(Z), \\ Z(0) = Z^*_{\text{spec}}, \end{cases} \tag{E_{auto}}$$

where I define the function $\mathcal{F}^{c=0}(Z) := 2g\left[\frac{\rho(Z)-\frac{1}{\rho(Z)}}{\rho(Z)+\frac{1}{\rho(Z)}} - Z\right]$ that does not depend directly on the environmental change. In line with the biological interpretation of (S_0) detailed in the last subsection, the function $\mathcal{F}^{c=0}$ can be interpreted as the **selection gradient under stable environment**. Note that the trait variance does not appear because it has been scaled to 1 in the considered time scale.

The dynamics described by autonomous equations such as (E_{auto}) are conveniently studied through their phase line, which is the graph of the function $Z \mapsto -c + \mathcal{F}^{c=0}(Z)$ (right-hand side of (E_{auto})). When it is positive (resp. negative), $Z(t)$ increases (resp. decreases), so the equilibria are located where it vanishes (they are stable when the slope is negative and unstable when it is positive). Notice that the only impact of the changing environment is a vertical translation of the phase-line under stable environment (positive values of c correspond to downward translations). This implies that it can drive some stable-environment equilibria to disappear or to shift. More precisely, the new equilibrium obtained from the initial specialist state is located at the rightmost intersection of the downward-shifted phase line and the x-axis that has a negative slope (see Fig. 2 for an illustration). This graphical identification of the equilibria of (E_{auto}) allows bypassing the lack of explicit analytical expressions for the equilibria analogous to the ones found in Section 4 of Dekens (2022). Here, the changing environment breaks the symmetry of the system that was algebraically instrumental in Dekens (2022), which renders (E_{auto}) too convoluted to be fully analysed.

3. Results

Under a fixed environment ($c = 0$) and in the parameter range where a specialist species exists and is viable ($[1 + 2m < 5g] \wedge [g(m-1) < m^2]$), the analysis done in Dekens (2022) shows that the selection gradient under stable environment $\mathcal{F}^{c=0}$ vanishes three times: in $-Z^*_{\text{spec}}$, 0 and Z^*_{spec}, with negative, positive and negative slopes respectively (see Fig. 2(a)). This means that there exist three equilibria: two mirrored stable equilibria describing specialization to each habitat with respective mean traits $-Z^*_{\text{spec}}$ and Z^*_{spec}, separated by an unstable equilibrium describing a generalist species (equally maladapted to both habitats). To understand the impact of a changing environment on the long-term adaptation of the focal species, I describe below the effect of increasing environmental speeds and increasing selection strengths on these equilibria. In my illustrations (Figs. 3, 5 and 6), I keep a constant intermediate migration rate for the sake of clarity ($m = 0.5$). I address sensitivity issues by displaying the analogous figures for a lower migration rate ($m = 0.2$) in Appendix K. I also test the results derived in this section with those from individual-based simulations in Appendix J (see in particular Fig. 7) to account for the influence of sampling effects and random demographic fluctuations.

3.1. Small environmental change: lagging behind the native habitat and beneficial loss of specialization?

For small environmental change speeds, the phase line indicates that the metapopulation's mean trait at equilibrium Z^* lags behind the initial value Z^*_{spec} and thus its distance from the native habitat's optimum (set at 1) increases. This is reminiscent of single-habitat models (see Kopp and Matuszewski (2014) for a review). However, contrary to single-habitat models where lagging is always deleterious for population size, this can lead to an increase of metapopulation size for small enough environmental change speeds. In fact, I show in Appendix C that, for the transient dynamics at all environmental speeds, the metapopulation size actually increases immediately after the start of the environmental shift (at $t \approx 0$), as the mean trait Z starts decreasing from Z^*_{spec}. This initial increase in metapopulation size occurs because when the mean trait Z^* starts lagging behind its initial value, it actually becomes closer to the refugium's optimum. The immediate loss of population in the native habitat is therefore overcompensated by the immediate gain of population in the refugium (even if it remains small), because the increase in adaptation for a trait far from an optimum is greater than the loss closer to an optimum when the selection functions are quadratic. This effect relies quite heavily on the precise shape of the selection functions, in particular their tails (for example, it does not occur when the selection functions are linear). The initial increase does not last, as, eventually, the lag with the native habitat increases and the increased adaptation to the refugium is not enough to compensate for the decreased adaptation to the native habitat.

A related phenomenon is that, for very small speeds of environmental change, the metapopulation moves to an equilibrium $Z^* \lesssim Z^*_{\text{spec}}$ for which its size is actually greater than its initial size. The population as a whole is less specialized to the native habitat and benefits from relative adaptation to the refugium.

3.2. Abrupt switch from the native habitat to the refugium: tipping point

In the last paragraph we explained that while for small environmental changes, the metapopulation can actually increase, it eventually starts dropping as the lag increases. However, as opposed to the single-habitat model, the path to extinction here is not straight-forward because of the existence of the refugium. I will first describe how this impacts the new equilibrium that is reached by the metapopulation, and then what can occur at the transient dynamics level on the path to this equilibrium.

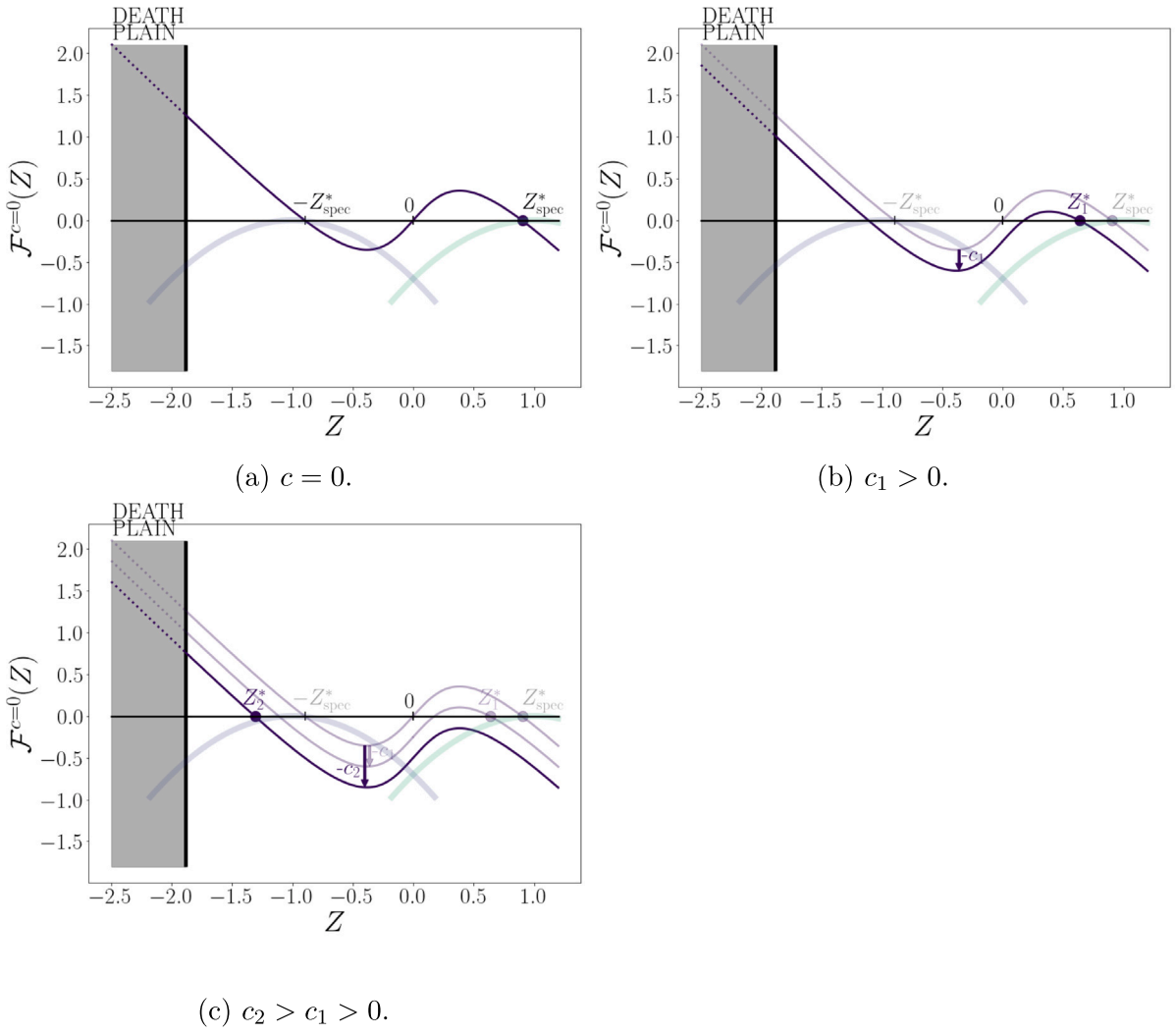

Fig. 2. Illustration of the selection gradient's phase line (purple dark line) (E_{auto}) for several environmental speeds (top left: stable environment $c = 0$, top right: environmental speed $c_1 > 0$, bottom left: environmental speed $c_2 > c_1 > 0$; for all subfigures: $g = 0.7, m = 0.5$). The local quadratic selection functions are indicated by the thick faded blue (refugium) and green (native habitat) curves. The grey area called the "Death Plain" refers to a non-viable region (where a metapopulation with such a mean trait has negative growth rate at low density). In each subfigure, the mean trait at equilibrium under a changing environment at a given speed is indicated by a filled circle (resp. Z^*_{spec}, Z^*_1 and Z^*_2). Notice how Z^*_1 remains quite close to the initial state under stable environment Z^*_{spec} (Fig. 2(b)), while Z^*_2 is far from it, closer to the refugium's optimum than to the native habitat's one (Fig. 2(c)).

New equilibrium. To determine the new equilibrium state reached by the population when the environment changes at speed c, one has to study the downward shifted phase line. As the phase line is smooth, it reaches a maximum value into $[0, 1]$. I call this maximum value $c_{\text{switch}} := \max_{Z \in [0, Z^*_{\text{spec}}]} \mathcal{F}^{c=0}(Z)$, which is reached when $Z = Z_{\text{switch}} > 0$. This means that, for environmental change's speeds that are lower $c \leq c_{\text{switch}}$, the metapopulation mean trait reaches an equilibrium value Z^* that is between Z_{switch} and Z^*_{spec} and thus closer from the native habitat's optimum than the refugium's one. Consequently, the metapopulation still retains a majority in the native habitat. However, for environmental change's speeds that are greater than c_{switch}, the metapopulation cannot reach an equilibrium with a positive mean trait Z^*, as the phase line resulting from a downward translation does not cancel into $[0, 1]$ anymore (see an example in Fig. 2(c)). In our case, the only stable equilibrium that is left corresponds to a mean trait Z^* that is negative and even lower than $-Z^*_{\text{spec}}$, which is the mean trait of a metapopulation specialized to the refugium under a stable environment ($c = 0$). This means that *the metapopulation completely reverses its habitat preference* and now lags behind $-Z^*_{\text{spec}}$, and becomes relatively better adapted to the refugium. *This shift from native habitat to refugium is abrupt*, because increasing the environmental speed even slightly above c_{switch} makes the possibility of remaining mainly in the native habitat completely disappear (see an illustration in Fig. 3(a)).

Remark 3.1. The critical speed of habitat switch c_{switch} is defined implicitly as the maximum value of $\mathcal{F}^{c=0}(Z)$ over a closed interval. Obtaining an explicit analytical expression requires maximizing the selection gradient under stable environment $\mathcal{F}^{c=0}(Z)$ with the (independent) constraint $P_Z(\rho) = 0$ coming from the ecological equilibrium. It is therefore too convoluted to be displayed here.

Tipping point. Once the metapopulation's mean trait has dropped abruptly below $-Z^*_{\text{spec}}$, lowering the speed of environmental change back under c_{switch} (ie. translating the phase line slightly upward) does not result in the reversal of the habitat switch. The metapopulation is now trapped in the basin of stability of specialization to the refugium. This indicates that the mean trait in the metapopulation has crossed a tipping point: for the metapopulation to become specialized to the native habitat again, the environment needs to actually change in the other direction, passing from a speed c_{switch} to a speed $-c_{\text{switch}}$ (because $\mathcal{F}^{c=0}$ is antisymmetric, see Appendix B).

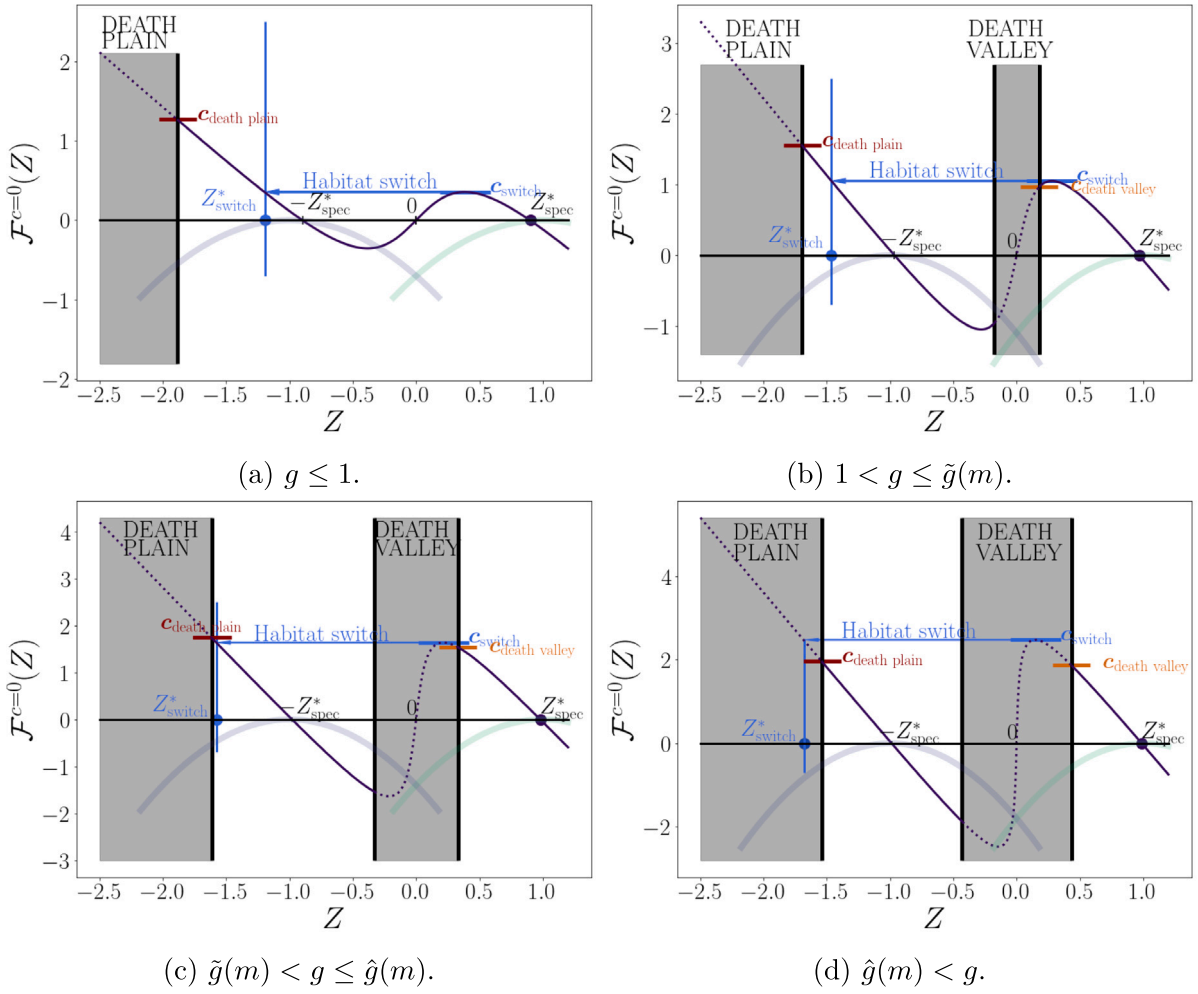

Fig. 3. Critical transition speeds for increasing selection with $m = 0.5$ (from top to bottom, left to right, $g = 0.7, 1.1, 1.4, 1.8$). The tipping point provoking a habitat switch ($c_{\text{switch}} = \max_{Z\in[0,Z^*_{\text{spec}}]} \mathcal{F}^{c=0}(Z)$) is indicated in blue, and the speeds corresponding to the non-viability area are indicated in orange ($c_{\text{death valley}}$) and in crimson ($c_{\text{death plain}}$). Below $g = 1$, the death valley does not exist (Fig. 3(a)). Between 1 and $\tilde{g}(m)$, the switch occurs before entering the death valley (Fig. 3(b)). For $g > \tilde{g}(m)$, the switch occurs within the death valley. Below $\hat{g}(m)$, the switch brings to a viable equilibrium (Fig. 3(c)) whereas it leads to extinction above (Fig. 3(d)).

Transient dynamics of the habitat switch. From the previous paragraphs, we know that the metapopulation will switch from mainly inhabiting the native habitat to the refugium when $c \geq c_{\text{switch}}$, because the new equilibrium is below $-Z^*_{\text{spec}}$. However, the latter does not describe the transient trajectory of the species during the switch. To do so, I will distinguish between two cases: intermediate selection ($\frac{1+2m}{5} < g < 1$) and strong selection ($g > 1$).

1. **Intermediate selection** ($\frac{1+2m}{5} < g < 1$): in this case, the viability analysis done in Proposition 3.1 of Dekens (2022) shows that the whole path of the mean trait $Z(t)$ (from lagging behind Z^*_{spec} to lagging behind $-Z^*_{\text{spec}}$) is viable. This means that for each $Z \in [-Z^*_{\text{spec}}, Z^*_{\text{spec}}]$, the metapopulation size $N(Z)$ (defined through the ratio $\rho(Z)$ satisfying the first line of (S_0), see the details in C e.g.) is positive. This occurs because the selection is not strong enough for the local growth rates at low density to both be negative at any given mean trait of the metapopulation $Z \in [-Z^*_{\text{spec}}, Z^*_{\text{spec}}]$. An example of this configuration is displayed in Fig. 3(a).
2. **Strong selection** ($g > 1$): in this case, the viability analysis done in Proposition 3.1 of Dekens (2022) shows that the converse happens. The path from the native habitat's optimum to the refugium crosses a non-viable stretch in the middle, that I call the *death valley*. The death valley extends from $-Z_{\text{death valley}}$ to $Z_{\text{death valley}}$, where

$$Z_{\text{death valley}} = \sqrt{\frac{(g+1-m)}{g} - \sqrt{\frac{1}{g^2}\left[m^2 - 4g\,(m-1)\right]}} > 0. \qquad (2)$$

Notice that, as the environmental change does not directly affect the subpopulation sizes, it also does not affect $Z_{\text{death valley}}$, ie the boundaries of the death valley (see for example Fig. 3(b)). The corresponding speed of environmental change $c_{\text{death valley}}$ is given by (see Appendix D for the derivation):

$$c_{\text{death valley}} = 2g Z_{\text{death valley}} \left(\frac{2}{Z^2_{\text{death valley}} + 1 + \frac{m-1}{g}} - 1 \right). \qquad (3)$$

My aim here is to describe accurately the population dynamics within the death valley. To do so, I need to distinguish between the two settings as stated in Remark 2.1. Indeed, the keen reader would have observed that *the death valley is a region where the population is not viable*, thereby the convergence of solutions of (S_ε) to solutions of (S_0) is not ensured. As a result, substantial discrepancies between the two models can occur. We highlight the differences by comparing the dynamics of the limit system (S_0) (dashed curves on Fig. 4) with the dynamics of the system (P_ε) with small positive within-family variance $\varepsilon > 0$ (plain curves on Fig. 4).

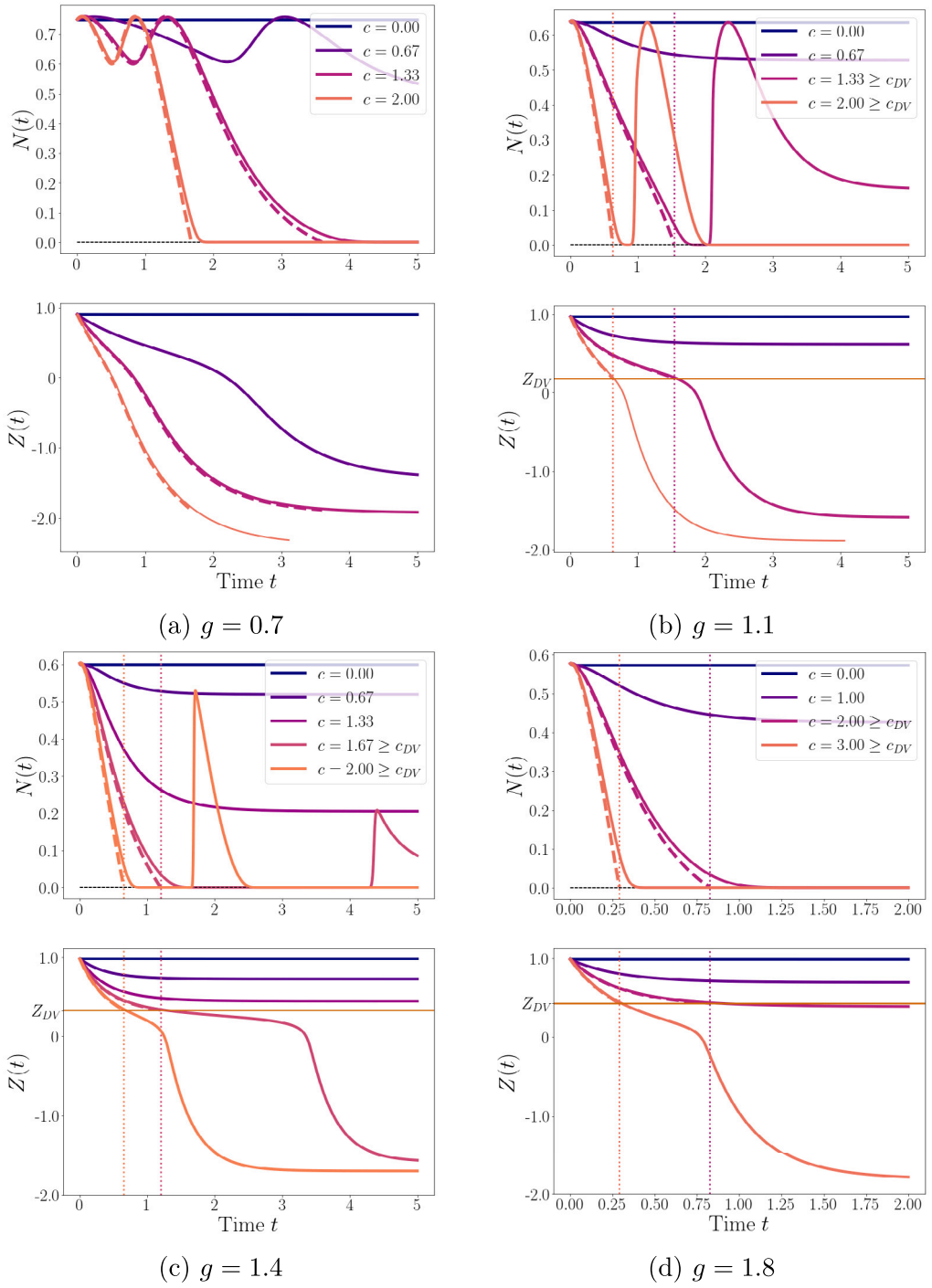

Fig. 4. Transient dynamics of the metapopulation's size $N(t)$ (upper panel) and mean trait $Z(t)$ (lower panel), for increasing environmental change speeds (dark to light colours, one out of three of those in Fig. 5) and increasing selection strengths corresponding to the ones used in Fig. 3 (left to right, top to bottom quadrants: $g = 0.7, 1.1, 1.4, 1.8$; with $m = 0.5$). The solid lines correspond to the dynamics given by (P_ε) with $\varepsilon = 0.05$, whereas the dashed ones correspond to the dynamics according to (S_0). In Fig. 4(b), Fig. 4(c) and Fig. 4(d), the thin horizontal lines labelled Z_{DV} in the lower panels indicate the value of $Z_{\text{death valley}}$. The thin vertical dotted lines in both panels indicate the entry time to the death valley given different speeds $c \geq c_{\text{death valley}}$.

Under the limit model (S_0), the dynamics within the death valley are straightforward: the population goes extinct as soon as its mean trait Z reaches the death valley and the habitat switch cannot occur. The system (S_0) follows the condition $\rho(t) > f_1(Z(t))$ (ensuring the viability of the metapopulation), which is violated as soon as the metapopulation's mean trait enters the death valley (see the dynamics represented with dashed lines in Fig. 4(b), Fig. 4(c) and Fig. 4(d) - the entry times to the death valley correspond to the vertical dotted lines). This means that, at this time, the metapopulation goes extinct.

However, numerical resolutions of (P_ε) with a small and positive within-family variance parameter $\varepsilon = 0.05$ paint a different and more nuanced picture. Approximately when the population enters the death valley ($Z_\varepsilon \approx Z_{\text{death valley}}$), the population size collapses to very low levels. However, *the population survives and*

its mean trait keeps evolving towards lower values. It will eventually exit the death valley, leading to a rebound of the population (see the dynamics represented with solid lines in Fig. 4(b) and Fig. 4(c) - the metapopulation size rebounds are located after the vertical dotted lines). These features of the joint trajectory of the population size and of its mean trait are typical of the phenomenon of *evolutionary rescue* (Holt et al., 2003). But how should one interpret it? Although the precise mathematical analysis is challenging to derive, here is an attempt to unpack the intuition behind these dynamics.

When $Z_\varepsilon(t)$ enters the death valley, the growth rate of the metapopulation at low density becomes negative. As a result, its size declines exponentially towards extinction. Since we consider here an environmental change with speed $c \geq c_{\text{switch}}$, the new equilibrium lies beyond the death valley (because it lies beyond the refugium's optimum). As such, it attracts the mean trait $Z_\varepsilon(t)$ from the beginning of the transient trajectory. $Z_\varepsilon(t)$ therefore enters the death valley while going through a habitat switch (for $c \geq c_{\text{switch}}$). This implies that the switch occurs and forces the mean trait $Z_\varepsilon(t)$ to cross the death valley. What follows is a race between the metapopulation' mean trait $Z_\varepsilon(t)$ exiting the death valley before the metapopulation goes extinct. In our deterministic model where the metapopulation can survive even at very low sizes (an extreme example is displayed with $c = 1.67$ in Fig. 4(c)), the mean trait always succeeds in exiting the death valley before extinction, so the metapopulation size eventually bounces back, primarily in the refugium (at least for some time). These two types of dynamics given on the one hand by the limit system (S_0) and on the other hand by (P_ε) are strikingly different. The analysis of the former indicates that the death valley cannot be crossed, ensuring immediate extinction as soon as the metapopulation's mean trait enters it. In contrast, numerical simulations of the latter suggest that the metapopulation always manages to linger on at low levels while its mean trait crosses the death valley, leading to evolutionary rescue. How can we make sense of this discrepancy? Since the behaviour of the metapopulation at low density appears to be instrumental, I have used stochastic individual-based simulations (presented in Appendix J) to clarify the conclusions. Their result is interestingly in-between the two deterministic predictions derived from (S_0) and (P_ε). Indeed, while the majority of stochastic trajectories do go extinct in the death valley (black squares between the orange and red ticks in Fig. 7(d)), a number of them do not (corresponding to the black circles in Fig. 7(d)) and their final state is well predicted by the phase line analysis once in the refugium (corresponding to the blue line in Fig. 7(d)).

3.3. Critical speed of environmental change for extinction

A crucial quantity in single-habitat models of adaptation to an environmental shift is the *critical speed of environmental change for persistence*, below which the environmental changes slowly enough for the population to adapt and persist, and above which it changes too fast and the population goes extinct. In the two-habitats framework that I consider here, persistence is not as clear-cut, as I will highlight cases in what follows where intermediate environmental speeds can lead to extinction. Instead, I thus use here *the critical speed of environmental change for extinction* c_{extinct} as the smallest speed such that $\forall c \geq c_{\text{extinct}}$, the population goes extinct at equilibrium. In this section, I give an explicit expression for c_{extinct}.

To do so, I rely once more on the viability analysis under a stable environment in Section 3.2 of Dekens (2022). It indicates that there exists a lower bound that I call $Z_{\text{death plain}}$, below which the metapopulation's mean trait Z always leads to negative growth rates at low density (leading to extinction), where:

$$Z_{\text{death plain}} = -\sqrt{\frac{(g+1-m)}{g} + \sqrt{\frac{1}{g^2}\left[m^2 - 4g(m-1)\right]}}. \tag{4}$$

This lower bound $Z_{\text{death plain}} < 0$ defines a corresponding environmental speed $c_{\text{death plain}} := \mathcal{F}^{c=0}(Z_{\text{death plain}})$ whose analytical expression reads (see a proof in D):

$$c_{\text{death plain}} = 2g Z_{\text{death plain}} \left(\frac{2}{Z^2_{\text{death plain}} + 1 + \frac{m-1}{g}} - 1 \right). \tag{5}$$

At this point, similarly as in Section 3.2, I need to separately present the results derived from the dynamics of the system (P_ε) which considers a small and positive within-family variance ε^2 and the ones derived from the dynamics of the limit system (S_0). As I explained in Section 3.2, the metapopulation always goes extinct when switching through the death valley according to (S_0) while this does not need to be the case according to (P_ε). This discrepancy naturally results in a discrepancy in the critical speed for extinction between the two settings, shown in Fig. 6 (solid black line for (P_ε) and dashed black line for (S_0)). I will discuss how to connect the two sets of results using the results of additional individual-based simulations that I conducted (Appendix J).

Critical speed of environmental change according to (P_ε). From the phase-line analysis of (E_{auto}), there exists a selection strength threshold $\hat{g}(m) > 1$ defined such that $c_{\text{switch}} \leq c_{\text{death plain}}$ below and conversely above (the explicit expression $\hat{g}(m)$ is too convoluted to be displayed for the same reason stated for c_{switch} in Remark 3.1, but it is graphically represented by the rightmost vertical dotted line in Fig. 6). This selection strength threshold is instrumental in distinguishing between two cases:

1. $g \leq \hat{g}(m)$: for $c \in [c_{\text{switch}}, c_{\text{death plain}}]$, the metapopulation switches to the refugium and lags behind the local optimum, but closely enough that it manages to persist (see Fig. 3(a), Fig. 3(b) and Fig. 3(c)). For $c \geq c_{\text{death plain}}$, the lag in the refugium after the switch is too large and extinction occurs. *Therefore, in this case, the critical speed for extinction is* $c_{\textit{death plain}}$ (see Fig. 5(b), Fig. 5(d) and Fig. 5(f)).
   Moreover, even if it does not impact the critical speed for extinction, it should be noted that for some values of $1 < g < \hat{g}(m)$, extinction can also occur for intermediate environmental speeds c that are lower than the critical speed $c_{\text{death plain}}$. This happens when the closest new stable equilibrium is located within the death valley without the possibility to be rescued by a habitat switch, which requires $c_{\text{death valley}} \leq c < c_{\text{switch}}$. In this case, the population ends up being trapped in the death valley and goes extinct. This situation requires the selection strength g to be above a threshold dependent on the migration rate that I note $\tilde{g}(m) > 1$, defined as the one leading to $Z_{\text{death valley}} = Z_{\text{switch}}$. For lower selection strengths than $\tilde{g}(m)$, the switch occurs before the metapopulation's mean trait enters the death valley, while for larger ones, it occurs within the death valley. The analytical expression of $\tilde{g}(m)$ is too convoluted to be displayed similarly to that of c_{switch} (see Remark 3.1). However, it is graphically represented by the second vertical dotted line in Fig. 6.
2. if $g \geq \hat{g}(m) > 1$, we have $c_{\text{death plain}} < c_{\text{switch}}$. Additionally, I show in Appendix E that, when $g \geq 1$, the following inequality always holds: $c_{\text{death valley}} < c_{\text{death plain}}$. Therefore, the switch always occurs within the death valley ($0 < Z_{\text{switch}} < Z_{\text{death valley}}$). For $c \in [c_{\text{death valley}}, c_{\text{switch}}]$, the metapopulation is stuck within the death valley without the opportunity to switch and goes extinct similarly as described above. However, conclusions differ from the first case for $c \geq c_{\text{switch}}$: the switch towards the refugium does occur, but it brings the population to a equilibrium where the lag with respect to the refugium's optimum is too large and provokes extinction (see Fig. 3(d)). Therefore, *in this case, the critical speed for extinction is* $c_{\textit{death valley}}$ (see Fig. 5(h)).

It is noteworthy to highlight that, from the results described above, the critical speed of environmental change displays two key features

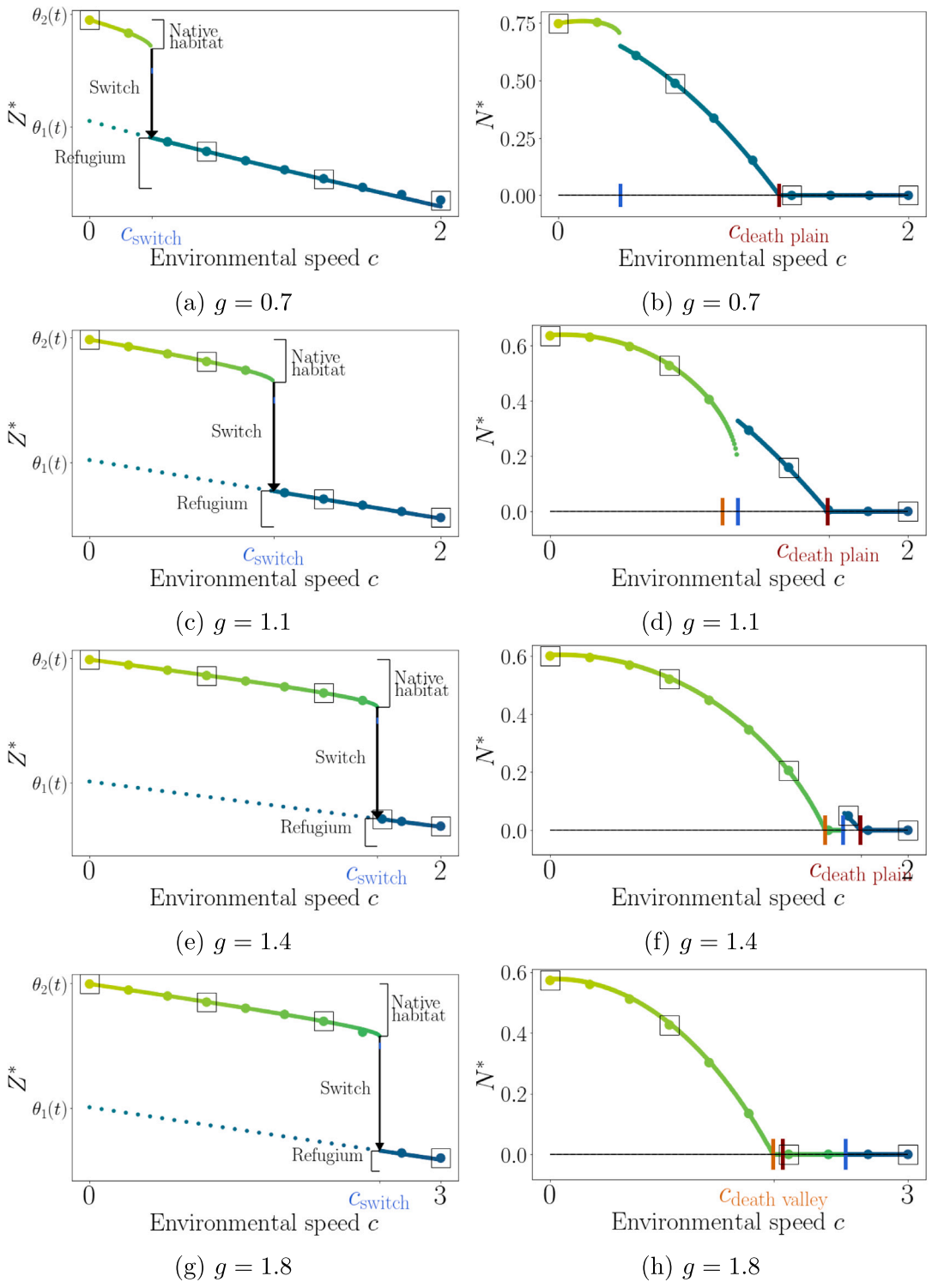

Fig. 5. Equilibrium mean trait Z^* (left panel) and metapopulation size N^* (right panel) as functions of the environmental speed c (x-axis), for increasing selection strengths corresponding to the ones used in Fig. 3 (top to bottom: $g = 0.7, 1.1, 1.4, 1.8$; with $m = 0.5$). Solid and dotted curves correspond to the analytical steady states given by (S_0) (green in the native habitat, blue in the refugium), and the large dots are given by end results of simulated numerical resolutions of (P_ε) with $\varepsilon = 0.05$. The squared dots indicate results from the simulations used in Fig. 4. The vertical ticks in the left panel's figures indicate c_{switch} (blue), $c_{\text{death plain}}$ (crimson) and $c_{\text{death valley}}$ (orange).

in this two-patch framework. It is discontinuous at $g = \hat{g}(m)$, because it jumps from $c_{\text{death plain}}$ ($g \leq \hat{g}(m)$) to $c_{\text{death valley}}$ ($g > \hat{g}(m)$), with $c_{\text{death valley}} < c_{\text{death plain}}$. Consequently, it is also non-increasing with respect to increasing selection (see Fig. 6).

Critical speed of environmental change according to (S_0). The main difference regarding the critical speed of environmental change between (P_ε) and (S_0) comes from the difference of behaviour with respect to the death valley.

As explained in Remark 2.1, the dynamics given by (P_ε) and (S_0) should be very similar on sections of the transient trajectories where the metapopulation is viable (thus where the convergence when $\varepsilon \to 0$ is ensured). Consequently, *when* $g < 1$ *(ie. when the death valley does not*

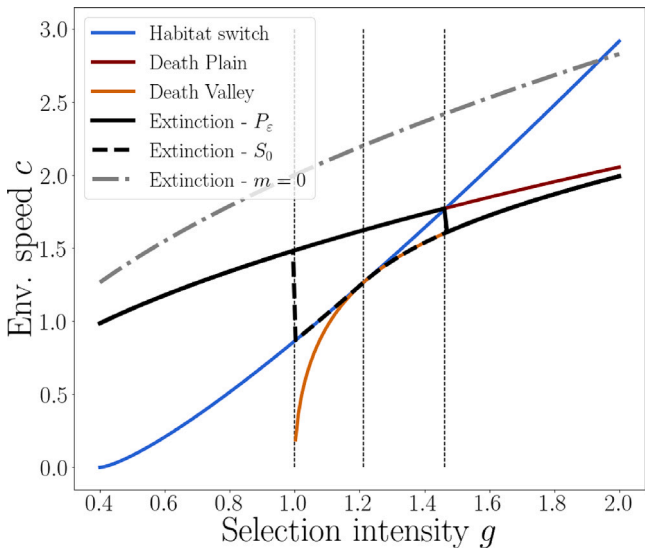

Fig. 6. Analytical predictions of the critical speed of environmental change with increasing selection (x-axis), with $m = 0.5$. The solid black line corresponds to the critical speed of environmental change according to the deterministic dynamics given by (P_ε) with a small within-family variance $\varepsilon > 0$, while the dashed black indicate the ones given by the limit system (S_0). The dichotomy between the two reflect the stochastic nature of the evolutionary rescue phenomenon (see the results of the IBS in Appendix J for an illustration). The coloured lines represent the different particular speeds that the analysis has identified and come from the analytical formula (3) for $c_{\text{death valley}}$ and (5) for $c_{\text{death plain}}$ and the identification of c_{switch} given in Section 3.2. The three vertical dotted lines delineate four selection regions corresponding to the ones illustrated in Figs. 3 and 5 ($g \leq 1$; $1 < g \leq \tilde{g}(m)$; $\tilde{g}(m) < g \leq \hat{g}(m)$ and $g > \hat{g}(m)$). The dotted–dashed grey line represents the critical speed of environmental change without migration, which coincides with the analogous quantity in single-habitats studies.

exist), the critical speed for environmental change according to (S_0) is the same as the one according to (P_ε), which is $c_{\text{death plain}}$.

However, there can potentially be significant discrepancies between the solutions of (P_ε) and (S_0) on parts of the transient trajectories where the metapopulation's growth rate at low density is negative and extinction is looming (thus where the convergence when $\varepsilon \to 0$ is not ensured). The latter is especially the case when the threat of extinction is only fleeting because the metapopulation only transiently crosses a non-viable stretch. One example is the case of the death valley's crossing, as explained in Section 3.2. Consequently, when $g \geq 1$ and the death valley does exist between the two habitats' optimal traits, the critical speed of environmental change according to (S_0) can be different from the one according to (P_ε):

1. if $1 \leq g \leq \tilde{g}(m)$: in this case, when $c \geq c_{\text{switch}}$, the habitat switch starts in a viable region ahead of entering the death valley ($Z_{\text{switch}} \geq Z_{\text{death valley}}$). However, as the habitat switch unfolds, the metapopulation's mean trait reaches the death valley and extinction occurs. As a result the critical speed of environmental change is lower than c_{switch}. Moreover, for $c < c_{\text{switch}}$, the new equilibrium is located between the initial state (Z^*_{asym}) and the threshold corresponding to the habitat switch $Z_{\text{switch}} < Z^*_{\text{asym}}$. Since the death valley upper boundary is lower than Z_{switch} for $1 \leq g \leq \tilde{g}(m)$, the new equilibrium is viable and the metapopulation persists.
   Consequently, *the critical speed of environmental change for $1 \leq g \leq \tilde{g}(m)$ is c_{switch}.*
2. if $g \geq \tilde{g}(m)$: in this case, the habitat switch, if it happens, starts within the death valley ($-Z_{\text{death valley}} < Z_{\text{switch}} \leq Z_{\text{death valley}}$). Moreover, as c_{switch} is defined as the maximal value of $\mathcal{F}^{c=0}$ on $[0,1]$ and $c_{\text{death valley}} = \mathcal{F}^{c=0}(Z_{\text{death valley}})$ with $Z_{\text{death valley}} \in [0,1]$, we have $c_{\text{death valley}} \leq c_{\text{switch}}$. This implies that, for $c \geq c_{\text{death valley}}$, the metapopulation's mean trait enters at one point in the death valley and extinction follows. Conversely, for $c \leq c_{\text{death valley}}$, the metapopulation lags behind the native habitat's optimal trait in a viable manner without switching (because $c \leq c_{\text{death valley}} \leq c_{\text{switch}}$). Therefore, *if $g \geq \tilde{g}(m)$, the critical speed of environmental change is $c_{death\ valley}$.*

Similarly, as highlighted in the last paragraph regarding (P_ε), *the critical speed of environmental change here is also discontinuous and non-increasing with respect to the selection strength* (jumping from $c_{\text{death valley}}$ to c_{switch} at $g = 1$).

Connecting the two-faced results of (P_ε) and (S_0) thanks to individual-based simulations (Appendix J). The findings of the last two paragraphs detailing the critical speed of environmental change are noticeably different between (P_ε) and (S_0). This can be better visualized in Fig. 6 by the discrepancy between the black solid line (representing the critical speed according to (P_ε)) and the black dashed line (same according to (S_0)). The only difference is when the selection strength g is between 1 (appearance of the death valley) and $\hat{g}(m)$, above which (P_ε) and (S_0) agree on the critical speed being $c_{\text{death valley}}$. This is due to the fact that the transient trajectories of (P_ε) and (S_0) handle the crossing (or not) of the death valley very differently, as explained in Section 3.2 and illustrated in Fig. 4(b) and Fig. 4(c).

However, one could argue that on the contrary, with regard to Fig. 5, both (P_ε) and (S_0) seem to agree on the equilibrium metapopulation size (right panel) and mean trait (left panel). What is going on there? The subtlety is that the solid lines in Fig. 5 do not represent the end point of dynamics given by (S_0), but rather the steady states cancelling the l.h.s of the differential equation featured in (S_0), irrespective of whether they can be reached from the considered initial state. Remember that, according to Remark 2.1, the convergence of solutions of (S_ε) towards solutions of (S_0) is actually ensured on parts of the transient trajectories where the solutions describe a viable metapopulation. Imagine that the initial point of the dynamics was the start of the metapopulation's rebound after crossing the death valley according to (P_ε). Then, in this situation, the solutions of (S_0) and (P_ε) would agree on the whole trajectory and the equilibrium state of the metapopulation according to (P_ε) would be well approximated by the one according to (S_0). It is thus the crossing of the death valley during the transient trajectories that introduces the discrepancy on the critical speeds given by (P_ε) and (S_0). Specifically, this discrepancy is due to how fleeting extinctions (when the metapopulation' size stays very low for some time) are handled by both settings.

The stochastic individual-based simulations (subsequently denoted IBS) that I performed with the same parameters as in Fig. 5 and that are presented in Appendix J shed some useful insights on the latter aspect. Indeed, they should be close to (P_ε) when the metapopulation size is large. Their results are summarized in a similar figure to Fig. 5, but where the numerical final states of the deterministic dynamics following (P_ε) are replaced by the final states of the IBS Fig. 7. Moreover, I display the median final metapopulation' size both between all replicate simulations (black squares) and between replicate simulations where the metapopulation persists (black circles), as well as the full variance between replicates (vertical black lines). For most sets of parameters, this distinction between replicates where the metapopulation persists versus all replicates does not matter and is not visible. However, one can observe that in Fig. 7(d), the two are not necessarily the same. For intermediate speeds of environmental change, while the majority of replicates do go extinct (black squares on the x-axis), the final states of the ones that persist (black circles on the blue line) are well predicted by the coloured lines corresponding to steady states of (S_0). They also match the final states of the corresponding numerical resolutions of (P_ε). This helps connect the results derived from the system with a small but positive within-family variance (P_ε) and from the asymptotic one (S_0). The dichotomy between their results exactly reflects the dichotomy between the possible steady states according to a stochastic version of the model. *When the crossing of the death valley*

is involved, the steady states of (P_ε) *match the steady states of stochastic dynamics conditioned on persistence, whereas the ones of* (S_0) *match the steady states of stochastic dynamics conditioned on extinction*. As soon as there is some within-family variance, albeit very small as in (P_ε), there is a chance that in the declining population, a few individuals are born with traits that are exceptionally fit to cross the death valley. At the limit of vanishing variance as in (S_0), the lack of variance annihilates this chance and the metapopulation never crosses the death valley. *Consequently, the two deterministic settings capture a different feature of the stochastic dynamics at low metapopulation's size within the death valley (optimistic and pessimistic)*. Ultimately, this questions the well-posedness of the critical speed of environmental change in this two-habitat framework that can exhibit two-faced dynamics of adaptation to changing environment.

3.4. Comparison with results from single-habitat models

Lagging behind the refugium. From the previous section, if $c \geq c_{switch}$, the metapopulation switches from lagging behind the native habitat ($0 < Z^* < Z^*_{\text{spec}} < 1$) to lagging behind the refugium ($Z^* < -1 < Z^*_{\text{spec}}$). The two configurations are not symmetrical. In the former situation, the metapopulation's mean trait is between the two local optima, so the situation is a compromise between adapting to the native habitat or the refugium. However, in the latter situation, adaptation to the native habitat is extremely poor and the metapopulation relies entirely on the refugium, at least when the migration is not too strong, e.g. $m \leq 1$. It is therefore reasonable to assume that the ratio between the subpopulation sizes reflect this: ie $\rho^* = \frac{N_2^*}{N_1^*} \ll 1$ (this is hinted by the monotony of $Z \mapsto \rho(Z)$ with quadratic selection functions, see Appendix I). Using this in the right-hand side of the second line of (S_0) leads to *an approximation of the lag of* Z^* *behind the refugium's optimum* (-1):

$$-1 - Z^* \underset{\leq}{\approx} \frac{c}{2g}. \tag{6}$$

Simulations suggest that this approximation is quite accurate, as the native habitat's influence on the metapopulation has almost completely faded, and *the analysis now connects to the single-habitat framework applied to the refugium, in which the lag is exactly the left-hand side of* (6) (see Kopp and Matuszewski (2014) and recall that the population variance in trait is here rescaled to 1 in the considered timescale and that the width of the fitness function is $\frac{1}{2g}$).

The cost of dispersal. Although the mean trait's lag behind the refugium's optimum once the switch has occurred ($c \geq c_{\text{switch}}$) is similar to the analogous quantity in a single-habitat framework, *the corresponding metapopulation size differs from its counterpart from single-habitat models as it is here burdened by the cost of dispersal* as well as to the selective cost due to the lag. To see this, let us assume that migration is not too strong $m \leq 1$. In this case, one can reasonably use the same assumption on the ratio between the subpopulation sizes as above: $\rho^* = \frac{N_2^*}{N_1^*} \ll 1$. The latter reflects the fact that, after the switch, the population in the native habitat is very small compared to the refugium's because it is extremely maladapted and inward migration is limited. Then, the total metapopulation size can be approximated by the size of the refugium's population: $N^* = N_1^* + N_2^* = N_1^*(1+\rho^*) \approx N_1^*$. Thus, using the expression of $N_1^* = m\rho^* - mf_1(Z^*)$ at equilibrium given by Lemma 1 of Dekens (2022), one can derive the following approximation:

$$\begin{aligned} N^* &\approx m\rho^* - mf_1(Z^*) \\ &= m\rho^* + 1 - g(Z^*+1)^2 - m \\ &\approx 1 - g(Z^*+1)^2 - m. \end{aligned}$$

The latter clearly suggests that the migration rate m directly lowers the metapopulation size as compared to the analogous quantity in a single-habitat.[1] Indeed, the latter would be equal to $1 - g(Z^*+1)^2$ (recall that the population's trait variance is rescaled to 1 in the considered timescale). The approximation of N^* above highlights the fact that random migration reliably makes the adaptation of specialist species to a fragmented environment more challenging than without migration. Indeed, even after the species has switched to specialize to the refugium, the constant back and forward migration continues. This means that a constant stream of individuals continues to migrate from the refugium to the native habitat where they are even more likely to die very shortly after arriving. This results effectively into a smaller metapopulation size compared to the case without migration ($m = 0$).

The cost of dispersal on the metapopulation's size logically impacts the critical speed for persistence. In Appendix G, I show that, all else being held equal, an increased migration rate directly leads to a lower critical speed of environmental change when $g \leq \hat{g}(m)$ (the evidence suggests the same when $g \geq \hat{g}(m)$ but is less direct). This occurs because the death plain extends further towards the refugium. More precisely, I show that

1. *the boundary of the death plain* $Z_{\text{death plain}}$ as defined by Eq. (4) *is an increasing function of the migration rate* m. As $Z_{\text{death plain}}$ is always negative, this effectively means that, when the migration rate increases, the death plain extends closer to the optimal trait in the refugium and the population's trait lag needs to be smaller for it to persist once the shift to the refugium has occurred.
2. *the critical environmental speed* $c_{\text{death plain}}$ *above which the population enters the death plain is a decreasing function of the migration rate* m. This means that, when the migration rate increases and the selection pressure g is kept fixed below $\hat{g}(m)$, the critical speed of environmental change is directly lowered (as it is equal to $c_{\text{death plain}}$ in this case, see Fig. 6) and the population can only persists in the refugium at smaller environmental speeds. When the selection pressure g is above $\hat{g}(m)$, the previous conclusion is not as straightforward, as in this case the critical speed for environmental change is $c_{\text{death valley}}$, not $c_{\text{death plain}}$. However, as shown in Appendix E, $c_{\text{death valley}}$ is always lower than $c_{\text{death plain}}$, while the difference between the two vanishes when g becomes large (and $m \leq 1$ - see Appendix F). This suggests that $c_{\text{death valley}}$ globally follows the same decreasing trend with respect to the migration rate when g is large enough. For consistency's sake, I lastly compute that both $c_{\text{death plain}}$ and $c_{\text{death valley}}$ (when $g \geq 1$) converge to the critical speed derived in single-habitats models when the migration rate vanishes.

There is a final non-intuitive layer to the effect of migration in fragmented and changing environments that I want to draw attention to. It concerns the metapopulation's mean trait instead of its size. The first paragraph of this section highlights that, when $g \leq \hat{g}(m)$, the equilibrium mean trait Z^* is approximately equal to $-1 - \frac{c}{2g}$ (where -1 is the optimal trait in the refugium). However, to draw a fair comparison to the case without migration, one should compare the latter to the equilibrium mean trait with respect to the native habitat, where the optimal trait is 1, leading to an equilibrium mean trait of $1 - \frac{c}{2g}$. This means that, *even if the metapopulation only persists for smaller speeds of environmental change in fragmented environments compared to if it were restricted to the sole native habitat, it explores a larger trait interval by switching to the refugium* (up to $-1 - \frac{c}{2g}$ versus $1 - \frac{c}{2g}$).

4. Discussion

Summary. In this work, a two-patch quantitative genetic model with moving optima was used to analyse the eco-evolutionary dynamics of

[1] One should however note that the accuracy of the approximation derived here becomes less clear when migration becomes strong, as the validity of the first assumption that $\rho^* \ll 1$ presumably deteriorates.

a sexually reproducing specialist species in a fragmented and changing environment consisting of its native habitat and a refugium. In a regime where the within-family variance is small, a separation of ecological and evolutionary time scales allows reducing the complexity of the analysis to a phase-line study of the selection gradient. First, I showed that small enough environmental speeds can actually be beneficial in terms of abundance thanks to a beneficial reduction of specialization. For larger environmental speeds, there exists an evolutionary tipping point corresponding to a sharp habitat switch from the native habitat to the refugium. With strong selection, this shift leads the population to cross a death valley between the two habitats' optima in trait space, where the population size temporarily plummets and possibly eventually rebounds (leading to evolutionary rescue). I finally compute the critical speed of environmental speed above which the population always goes extinct. This critical speed does not need to be increasing and can be discontinuous with respect to increasing selection strengths, especially with strong local selection.

Critical speed of environmental change: fragmented spatial structure versus single-habitat. In Section 3.3, I derived the critical speed of environmental change above which the population goes extinct because it is too maladapted as a whole. Because of the fragmented nature of the two-patch environment and the existence of the refugium, this critical speed differs in a number of ways as compared to the one classically derived in a single-habitat framework with quadratic selections (Lynch and Lande, 1993; Bürger and Lynch, 1995; Kopp and Matuszewski, 2014).

First, here, the analysis shows that increased selection strength does not always equate to the population tracking the changing environment more efficiently, as in a single habitat with a quadratic selection function. More precisely, above a selection threshold, the critical speed of environmental change decreases discontinuously from $c_{\text{death plain}}$ to $c_{\text{death valley}}$ (or potentially c_{switch}). This is due to the fact that with strong selection, the population can stay trapped within the rift between the habitats without begin able to switch. A related result (even though it does not impact the critical speed of environmental change) is that the population can go extinct for intermediate speeds of environmental change (ie. strictly below the critical speed), which does not occur with a single-habitat framework. Another striking difference is that here, the critical speed for environmental change can have two very different values for some sets of parameters depending on the interplay between within-family variance and stochastic demographic fluctuations at low density during the crossing of the death valley (see Section 3.3).

Moreover, one could be led to think that, because of the existence of the refugium, the population would be sheltered from extinction for larger environmental speeds than the critical speed derived in the analogous single-habitat models. Indeed, once the population has switched to lag behind the refugium, its adaptation is almost entirely determined by the dynamics within the refugium, as the migrants sent to the native habitat are too maladapted to make any significant contribution by gene flow. Therefore, the resulting dynamics are then very similar to the ones derived in the single-habitat framework, except for one major difference: the cost of dispersal, as highlighted by the results presented in Section 3.4. Indeed, I showed there that an increased migration rate reliably translates into a lower critical environmental speed for extinction. The intuition behind this lies in the constant back and forward migration between habitats. As the latter keeps on operating even after the species switches to specialize to the refugium, it effectively leads to a constant loss of population from the refugium that is not replenished. Thus, for a given lag in the refugium close to the critical one, the corresponding metapopulation size, approximated by the population size in the refugium, is actually smaller than without migration. Consequently, the critical environmental speed given by the present two-patch model is always lower than in single-habitat models.

Fragmented spatial structure with moving optima versus time-shifting environmental gradient in a continuous space. It would be tempting to use the present analysis as a literal stepping stone, by adding patches in a linear fashion in the hope of connecting the continuous space models of adaptation asymptotically to a time-shifting environmental gradient. However, I think that some caution is needed when passing at the limit, because the space granularity is instrumental to obtain the qualitative results of this study, especially with strong selection. Indeed, with strong selection, a death valley of negative growth rate at low density appears between the two habitats, which is a key feature of fragmented environments whose translation in the continuous space limit is all but clear. Nevertheless, here, it underpins a significant part of the most original results (the sharp dynamics of evolutionary rescue), but also the non-monotonicity of extinction (which can occur at lower environmental speeds than the critical one) and the discontinuous nature of the critical speed of environmental change with respect to increasing selection strength. The last two results differ from the results of quantitative genetics models considering an environmental gradient shifting at a constant speed in a continuous space framework (Pease et al., 1989; Polechová et al., 2009; Duputié et al., 2012; Aguilée et al., 2016; Alfaro et al., 2017). Indeed, all of them conclude that there exists a critical speed under which the population always persist and beyond which it goes extinct. Note that there exists some variation due to the particular framework of each studies: for example, the mean trait speed can be lower than the environmental speed (which does not happen here) due to long range pollen dispersal (Aguilée et al., 2016) or in the case of a steep environmental gradient leading to a limited range equilibrium (Polechová et al., 2009). However, in both cases, the critical speed remains continuous with respect to increasing selection strength at the transition between qualitatively different equilibria.

That said, one can draw some qualitative parallels between this study and the framework of Polechová et al. (2009). Indeed, the authors show that increasing the steepness of the environmental gradient (all else begin equal) leads from a uniform range equilibrium (where the species invade the whole space) to a limited range equilibrium (where the species only significantly persists in a bounded spatial range). This result is an extension of that obtained in the study of Kirkpatrick and Barton (1997) with stable environment (see also (Mirrahimi and Raoul, 2013; Raoul, 2017)). This echoes the passage from a generalist species equilibrium when selection is weak relative to migration ($g \leq 1+2m$) to a specialist species equilibrium when the converse holds ($g > 1+2m$) in the stable environment framework of Dekens (2022) (note that, here, the study exclusively focuses on the parameter range $g > 1 + 2m$ so on specialist species). However, as pointed out, the major difference is that the fragmented nature of the environment allows for sharp dynamics to occur that does not seem to exist in the continuous space viewpoint. Reconciling the two frameworks will require additional technical work.

Evolutionary tipping points in dynamics of structured populations. In Section 3.2, the analysis identifies tipping points in the dynamics of the population's mean trait that lead to sharp habitat switches. When the environmental speed is below a threshold c_{switch}, the population's mean trait lags behind the native habitat's optimum, but is closer from it than from the refugium's optimum. Therefore, the bulk of the population is still located in the native habitat. (Just) above the threshold, the population's mean trait shifts abruptly to lag behind the refugium's optimum, far from the native habitat's one. Consequently, the population is suddenly relatively better adapted to the refugium than to the native habitat. This sudden change of niche is difficult to reverse, because lowering the environmental speed just below the threshold will not restore the initial configuration, as the population remains "trapped" in the refugium's basin of stability. Restoring the population in its native habitat actually would require completely reversing the environmental change, with the opposite speed ($c_{\text{switch}} \to -c_{\text{switch}}$).

Mathematically, one can visualize and predict such a tipping point thanks to the phase line study described in Section 3.2. A tipping point

corresponds to a local maximum of the selection gradient (in our case the rightmost behind the initial mean trait). Assuming the selection gradient is smooth and non-constant, a sufficient analytical condition for the existence of a local maximum of the selection gradient is the co-existence of multiple equilibria (located where the selection gradient vanishes). This is in agreement with what occurs in a single-habitat framework under a changing environment with non-quadratic selection functions where maladaptation stabilizes away from the optimum (Osmond and Klausmeier, 2017, Garnier et al., 2023). Indeed, in this case, the selection gradient under stable environment vanishes at the optimal trait and converges to 0 in $-\infty$. Heuristically, this means that the situation with an infinite lag is an asymptotic equilibrium. Therefore, between $-\infty$ and the optimal trait, the selection gradient reaches a local maximum, which corresponds to the evolutionary tipping point identified in the aforementioned studies. In these cases, past the tipping point, the lag grows indefinitely, so the population abruptly becomes extinct. In the present work, this does not occur because the local selection functions are quadratic. Past the tipping point, the mean trait jumps on the stable branch of the selection gradient near the refugium's optimum, so the population switches habitats abruptly and the lag stabilizes behind the refugium's optimum. Moreover, here, either the jump brings the population to a viable state, or it was already extinct for environmental speeds just below the tipping point. So, in the present case, the evolutionary tipping point does not lead to an abrupt extinction. However, this lack of extinction following a tipping point might be strongly linked to the particular choice of quadratic selection functions used here.

To summarize, this work suggests that evolutionary tipping points can arise in stage-structured populations' dynamics because of non-monotonic selection gradients, even with quadratic selection functions. This feature might be facilitated by naturally existing feedback loops between demography and evolution in these kinds of models. Indeed, these lead to integrative optimal traits that depend on the demographic state of the system, itself a function of the evolutionary state. For example, in the present work, this optimal trait is $\frac{\rho(Z)-\frac{1}{\rho(Z)}}{\rho(Z)+\frac{1}{\rho(Z)}}$, where $\rho(Z) = \frac{N_2(Z)}{N_1(Z)}$ is the ratio between the two subpopulation sizes when the metapopulation mean trait is Z. A comparison with the analogous optimal trait obtained in the age-structured model (Cotto et al., 2019) suggests a correspondence between the elasticities quantifying the sensitivity of the population growth rate with respect to given transitions in their life cycle (introduced in Barfield et al., 2011) and the demographic terms $\rho(Z)$ and $\frac{1}{\rho(Z)}$ here. In our model, these quantities might thus be interpreted as being proportional to the elasticities linked to migration from one patch to the other. As such, they weight the two local optima to build an integrative optimal trait for global adaptation of the metapopulation. Therefore, linking evolutionary tipping points and adaptation of stage-structured populations might come down to understanding the influence of such integrative optimal traits that account for different components of fitness on the co-existence of multiple equilibria in the system.

Constrains in niche evolution and evolutionary rescue. The phenomenon of evolutionary rescue that is highlighted in Section 3.2 occurs because of the interplay between the sharp habitat switch and the existence of a death valley between the two local optima. This death valley is an area of the trait space (in our case, around $Z = 0$) where the growth rate at low density is negative and occurs when local stabilizing selection functions decline fast enough away from the optima. When the environmental speeds exceeds the threshold corresponding to the habitat switch, the mean trait is attracted to an equilibrium beyond the death valley. Therefore, during the habitat switch, the mean trait is led to cross the death valley. As soon as it steps in the death valley, the population size declines exponentially. Meanwhile, if there is even a little trait variance within the population (as per (P_ε)), the mean trait keeps decreasing to reach the lower bound of the death valley, where the growth rate at low density becomes positive again, which leads to a rebound of the population. Conversely, without variance (as per the limit model (S_0)), the population goes extinct within the valley. This death valley connects with the concept of "fundamental niche limits" in moving optimum models highlighted in the review of Klausmeier et al. (2020). In a changing environment, species can adapt not only by shifting its spatial distribution, but also by shifting its niche, like in Aguilée et al. (2016). However, it might happen that the niche is also biologically constrained, defining regions of positive and negative growth rate at low density (the latter in our case comprising the death valley). If the adaptive trajectory crosses such a region, the population size plummets, but can be saved if it comes back into the fundamental niche (see Fig. 6 of Klausmeier et al. (2020) for an illustration). It is noteworthy to point out that this phenomenon of evolutionary rescue, as in our case, does not rely on the advent of beneficial de novo mutations, rather on standing genetic variation within the population prior to entering the death valley. This standing genetic variation is due to the redundancy of the highly polygenic genetic architecture with numerous small effects that shift in frequency along the adaptive trajectory and segregate due to sexual reproduction.

Limits of the model. The deterministic model that I use allows working with clear assumptions in well-defined settings (P_ε) and (S_0). They thus lead to clear-cut results. However, these deterministic systems are not equipped to capture some finer phenomena, in particular those where the metapopulation size is very small, which makes stochasticity central. This is for example the case with the transient crossing of the death valley. As was hinted throughout Section 3, and especially in Section 3.2 and Section 3.3, my approach there shows some limits. I showed there that the discrepancies between the two sets of results derived from (P_ε) and (S_0) can be reconciled when considering the results of the supplementary individual-based simulations (IBS) that I performed originally to account for the influence of sampling effects and random demographic fluctuations (detailed in Appendix J). On the one hand, the results of the IBS are in excellent agreement with the numerical resolutions of (P_ε) as well as the analytical steady states of (S_0) whenever the equilibrium state of the population is either far from extinction, or definitely extinct. On the other hand, as the IBS are subject to random demographic fluctuations, they give a more nuanced conclusion than what either the models (P_ε) or (S_0) predict about the evolutionary rescue phenomenon across the death valley (always rescue according to the former and always extinction according to the latter). In fact, within the considered parameter range, the IBS show that the metapopulation does not get rescued in the majority of the replicate simulations, as predicted by the dynamics of (S_0). However, in some replicate simulations, it does, and then the IBS result in an equilibrium matching both the numerical results of (P_ε) and the steady states analysis of (S_0) (the latter being conditioned on having crossed the death valley — see Fig. 7(d)). This is because the crossing of the death valley requires exceptionally fit individuals, who could never have been born in the limit of vanishing within-family variance (underpinning (S_0)) and who are reliably born in the deterministic model (P_ε) with a small and positive within-family variance. In reality, this is modulated by chance and translates into a probability of rescue, which the IBS can give an estimation of (and which cannot be quantified by my approach).

To take matters even further than accounting for the influence of demographic stochasticity and sampling effects, one might focus on the central hypothesis of this model, namely about the within-family segregational variance. A key feature that makes the model analytically tractable is that the within-family segregational variance is fixed, therefore summarizing in one parameter all the details of the underlying genetic architecture (the IBS I performed make the same assumption in order to isolate the influence of population dynamics' stochasticity). A first direct consequence is that this model does not account for the biological constraints that a finite genetic architecture imposes on the

possible phenotypic range. The latter would be necessarily bounded and will be exceeded in the long run by a never-ending shifting optimum, making it impossible for the population to adapt without de novo mutations (connecting once again with the fundamental niche limits of Klausmeier et al. (2020)). Furthermore, it is known that in a finite population in a stable environment, this segregational variance becomes eroded by inbreeding through time (see Barton et al. (2017) for a quantification of the error that builds up). This is presumably enhanced during rescue events, where the population goes through a significant bottleneck, which is known to reduce the within-family genetic variance severely (or conversely, increase the probability of relatedness). The erosion of within-family variance is likely to drastically change the occurrence of evolutionary rescue across the death valley as can be hinted by the striking dichotomy between the dynamics of (P_ε) and (S_0) around the death valley (see Section 3.2 and Section 3.3). Specifically, whereas in (P_ε), the population picks up after an episode of rescue with the same segregational variance, allowing it to persist in the long run in some cases by stabilizing its lag with the refugium's optimum, I presume that stochastic individual-based simulations with explicit genetic architecture would show that an *extinction debt* can accumulate as a result of maladaptation and the loss of genetic variance, dooming the population quite soon after the rebound (relating to the concept introduced in Tilman et al. (1994)). Quantifying both the probability of evolutionary rescue and the long-term consequences of the loss of genetic variance would require adopting a stochastic modelling approach with an explicit genetic architecture.

Perspectives. As detailed above, a modelling choice that harbours the potential to significantly change the qualitative results of moving optimum quantitative genetic models is the one about the (local) selection function. Indeed, for example, in the single-habitat framework, Osmond and Klausmeier (2017), Klausmeier et al. (2020) and Garnier et al. (2023) highlight how choosing a selection function where maladaptation stabilizes away from the optimum instead of quadratic selection functions where maladaptation increases faster and faster away from the optimum leads to the occurrence of evolutionary tipping points. One can thus wonder how making similar choices would alter the results here and how to analyse a model with different selection functions. As a matter of fact, the analytical steps used in this study (justification of the Gaussian approximation of local trait distributions under small within-family variance and separation of ecological and evolutionary time scales leading to the phase line study) are robust to using other selection functions: I focused here on the quadratic case here because it permits derivation of explicit analytical results. With another choice of selection function, the precise expression and properties of the phase line linked to the selection gradient will depend on the particular choice and will potentially lead to qualitatively different results. However, the general method used here for analysing the resulting phase line is also transferable to another one arising from a different selection gradient.

The major hypothesis underpinning the analysis and therefore the results is that the within-family variance due to the segregation of the many small-effect loci underlying the adaptive quantitative trait is small compared to the distance between the local optima (but also more generally all the other parameters). This regime has been the analytical frame of several studies modelling trait inheritance with the infinitesimal model (Calvez et al., 2019; Patout, 2023; Garnier et al., 2023; Dekens, 2022). It provides sufficient standing genetic variance for selection to shift the population's mean trait, albeit on a slower time scale than the ecological dynamics governed by birth, death and migration processes, which allows one to justify the Gaussian approximation of local trait distribution that is classical for quantitative genetic models. As this hypothesis leads to the sharp dynamics presented in Section 3, one could ask what would happen if one relaxes this assumption. Beyond a purely theoretical question, this could have practical implications for conservation purposes: in the case of niche specialist species facing climate change, would it be beneficial to try and increase the standing genetic variance to promote local adaptation and would this make the species more resilient to greater environmental speeds? A further study is required to address this issue.

CRediT authorship contribution statement

Léonard Dekens: Writing – review & editing, Writing – original draft, Methodology, Investigation, Formal analysis, Conceptualization.

Data availability

The codes to reproduce the figures of this article are available at https://github.com/ldekens/two-patch-model-changing-environment.

Acknowledgements

I first thank Vincent Calvez and two anonymous reviewers for reviewing this manuscript and offering great suggestions to improve it, and Ophélie Ronce for initially introducing me to the biological question underlying this work and for subsequent insightful discussions. I also thank Sepideh Mirrahimi, Amandine Véber and Sally Otto for valuable feedback. I greatly thank Áine McColgan and James DiFrisco for language editing of the manuscript. I thank the Foundation for Mathematical Sciences in Paris (FSMP) for funding my work during my time at the MAP5 department of the Université Paris Cité in Paris. I also acknowledge having received partial funding from the ANR project DEEV ANR-20-CE40-0011-01 and from the European Research Council (ERC) under the European Union's Horizon 2020 research and innovation programme (grant agreement No 865711). This work was supported by the Francis Crick Institute, which receives its core funding from Cancer Research UK (CC2240), the UK Medical Research Council (CC2240), and the Wellcome Trust, United Kingdom (CC2240).

Appendix A. Detailed derivation of the limit system (S_0)

Dimensionless system. In the regime where the within-family variance $\boldsymbol{\sigma}^2$ is small compared to the difference between the local optima ($\boldsymbol{\theta_2} - \boldsymbol{\theta_1} = 2\boldsymbol{\theta}$), it is convenient to define the following rescaled variables and parameters to get a dimensionless system from $(\boldsymbol{P})$:

$$\varepsilon := \frac{\sqrt{2}\boldsymbol{\sigma}}{\boldsymbol{\theta}}, \quad t := \varepsilon^2 \boldsymbol{r} t, \quad z := \frac{\boldsymbol{z} - \boldsymbol{c}t}{\boldsymbol{\theta}}, \quad c := \frac{\boldsymbol{c}}{\varepsilon^2 \boldsymbol{r}\boldsymbol{\theta}}, \quad g := \frac{\boldsymbol{g}\boldsymbol{\theta}^2}{\boldsymbol{r}}, \\ m := \frac{\boldsymbol{m}}{\boldsymbol{r}}, n_{\varepsilon,i}(t,z) := \frac{\boldsymbol{\kappa}}{\boldsymbol{r}} \boldsymbol{n_i}(\boldsymbol{t},\boldsymbol{z}), \quad N_{\varepsilon,i}(t) = \frac{\boldsymbol{\kappa}}{\boldsymbol{r}} \boldsymbol{N_i}(\boldsymbol{t}), \tag{7}$$

and the infinitesimal model reproduction operator $\mathcal{B}_\varepsilon[n_{\varepsilon,i}](t,z) = \boldsymbol{\mathcal{B}_\sigma}[\boldsymbol{n_i}](\boldsymbol{t},\boldsymbol{z})$. Notice in particular that the time is rescaled according to the amount of small variance generated by reproduction events (of order $\frac{\varepsilon^2}{2}$). Rescaling $(\boldsymbol{P})$ according to (7) yields (P_ε) that I recall here for the sake of completeness:

$$\begin{cases} \varepsilon^2 \partial_t n_{\varepsilon,1}(t,z) - \varepsilon^2 c \partial_z n_{\varepsilon,1}(t,z) = \mathcal{B}_\varepsilon[n_{\varepsilon,1}](t,z) - g(z+1)^2 n_{\varepsilon,1}(t,z) \\ \qquad\qquad - N_{\varepsilon,1}(t) n_{\varepsilon,1}(t,z) + m\left(n_{\varepsilon,2}(t,z) - n_{\varepsilon_1}(t,z)\right), \\ \varepsilon^2 \partial_t n_{\varepsilon,2}(t,z) - \varepsilon^2 c \partial_z n_{\varepsilon,2}(t,z) = \mathcal{B}_\varepsilon[n_{\varepsilon,2}](t,z) - g(z-1)^2 n_{\varepsilon,2}(t,z) \\ \qquad\qquad - N_{\varepsilon,2}(t) n_{\varepsilon,2}(t,z) + m\left(n_{\varepsilon,1}(t,z) - n_{\varepsilon,2}(t,z)\right). \end{cases} \tag{P_ε}$$

The change in the trait variable $z := \frac{z - ct}{\theta}$ means that we place ourselves in the moving-frame reference that moves at the same speed as the environment. In this referential, the local optima are fixed, but the environmental shift's action appears in an additional advection term (where the factor ε^2 comes from the change in the time variable):

$$\partial_t \boldsymbol{n_i}(\boldsymbol{t},\boldsymbol{z}) = \varepsilon^2 \partial_t n_{\varepsilon,i}(t,z) - \boxed{\varepsilon^2 c \partial_z n_{\varepsilon,i}(t,z)}.$$

Moment-based system in the regime of small within-family variance. In this paragraph, I justify shifting the analysis from the full system (P_ε) describing the dynamics of the local trait distributions $n_{\varepsilon,1}(t,z), n_{\varepsilon,2}(t,z)$, to a moment-based system (M_ε) obtained from (P_ε) by integration and that describes the joint dynamics of the subpopulation sizes $N_{\varepsilon,1}(t)$, $N_{\varepsilon,2}(t)$ (obtained by applying the integral operator $\int_{\mathbb{R}} \cdot\, dz$ to (P_ε)) and the local mean traits $\overline{z}_{\varepsilon,1}(t), \overline{z}_{\varepsilon,2}(t)$ (with $\overline{z}_{\varepsilon,i}(t) := \int_{\mathbb{R}} z\, n_{i,\varepsilon}(t,z) dz$ in habitat i.) Indeed, in the regime of small within-family variance, Dekens (2022) showed that this moment-based system obtained by integration is closed, as the trait distributions $n_{\varepsilon,1}$ and $n_{\varepsilon,2}$ are both approximately Gaussian with a small variance $2\varepsilon^2$. The derivation of the moment-based system is similar as in Dekens (2022) for most terms, except for the advection term $-c\partial_z n_{\varepsilon,i}$ that comes from the changing environment. I detail its integration in what follows.

As the local distributions $n_{\varepsilon,i}$ are expected to stay concentrated, the speed of the environmental change does not directly impact the dynamics of the subpopulations sizes at the main order, as $\int_{\mathbb{R}} \partial_z n_{\varepsilon,i}(t,z) dz \approx 0$. However, it does impact directly the dynamics of the local mean traits, since one can integrate by parts to obtain

$$\frac{1}{N_{\varepsilon,i}} \int_{\mathbb{R}} c z \partial_z n_{\varepsilon,i}(t,z) dz \approx -\frac{c}{N_{\varepsilon,i}} \int_{\mathbb{R}} n_{\varepsilon,i}(t,z) dz = -c.$$

Due to the last computation, the moment-based system obtained from integrating (P_ε) here yields

$$\begin{cases} \varepsilon^2 \frac{dN_{\varepsilon,i}}{dt} = \left[1 - N_{\varepsilon,i}(t) - g(\overline{z}_{\varepsilon,i}(t) - (-1)^i)^2 - g\varepsilon^2\right] N_{\varepsilon,i}(t) \\ \qquad\qquad + m\left(N_{\varepsilon,j}(t) - N_{\varepsilon,i}(t)\right) + \mathcal{O}(\varepsilon^4), \\ \varepsilon^2 \frac{d\overline{z}_{\varepsilon,i}}{dt} = -\varepsilon^2 c + 2\varepsilon^2 g((-1)^i - \overline{z}_{\varepsilon,i}(t)) + m \frac{N_{\varepsilon,j}(t)}{N_{\varepsilon,i}(t)} (\overline{z}_{\varepsilon,j}(t) - \overline{z}_{\varepsilon,i}(t)) + \mathcal{O}(\varepsilon^4). \end{cases} \tag{M_ε}$$

Separation of time scales. Introducing the same slow–fast variables $\delta_\varepsilon := \frac{\overline{z}_{\varepsilon,2} - \overline{z}_{\varepsilon,1}}{2\varepsilon^2}$ (trait discrepancy between habitats) and $Z_\varepsilon := \frac{\overline{z}_{\varepsilon,2} + \overline{z}_{\varepsilon,1}}{2}$ (average trait in the metapopulation) and denoting by $\rho_\varepsilon > 0$ the ratio between subpopulation sizes: $\rho_\varepsilon := \frac{N_{2,\varepsilon}}{N_{1,\varepsilon}}$ as in Dekens (2022), one can obtain the following slow–fast system from (M_ε):

$$\begin{cases} \varepsilon^2 \frac{d}{dt} \begin{pmatrix} N_{\varepsilon,1} \\ N_{\varepsilon,2} \\ \delta_\varepsilon \end{pmatrix} = G(Z_\varepsilon, N_{\varepsilon,1}, N_{\varepsilon,2}, \delta_\varepsilon) + \varepsilon^2 \nu_{N,\varepsilon}(t), \\ \frac{dZ_\varepsilon}{dt} = -c + 2g\left[\frac{m}{2g}\delta_\varepsilon\left(\rho_\varepsilon - \frac{1}{\rho_\varepsilon}\right) - Z_\varepsilon\right] + \varepsilon^2 \nu_{Z,\varepsilon}(t), \\ (Z_\varepsilon(0), N_{\varepsilon,1}, N_{\varepsilon,2}, \delta_\varepsilon(0)) = \left(Z^*_{\text{spec}}, N^*_{1,\text{spec}}, N^*_{2,\text{spec}}, \delta^*_{\text{spec}}\right), \end{cases} \tag{S_ε}$$

where $\delta^*_{\text{spec}} := \frac{2g}{m}\left(\rho^*_{\text{spec}} + \frac{1}{\rho^*_{\text{spec}}}\right)^{-1}$, with $\rho^*_{\text{spec}} := \frac{N^*_{2,\text{spec}}}{N^*_{1,\text{spec}}}$.

Note that the term δ_ε, which represents the difference between the two local mean traits, directly involves the within-family variance small parameter ε^2 at its denominator. This highlights the fact that the two local mean traits are very close to one another in this regime. Moreover, the function $G : \mathbb{R} \times \left(\mathbb{R}^*_+\right)^2 \times \mathbb{R} \to \mathbb{R}^3$ and the residues $\nu_{N,\varepsilon}$ and $\nu_{Z,\varepsilon}$ are defined identically as in Dekens (2022) (Eq. (18)). In particular, G is defined according to the following (for $(Z, N_1, N_2, \delta) \in \mathbb{R} \times \left(\mathbb{R}^*_+\right)^2 \times \mathbb{R}$):

$$G(Z, N_1, N_2, \delta) = \begin{pmatrix} \left[1 - N_1 - g(Z+1)^2 - m\right] N_1 + m N_2 \\ \left[1 - N_2 - g(Z-1)^2 - m\right] N_2 + m N_1 \\ 2\, g - m\left(\frac{N_2}{N_1} + \frac{N_1}{N_2}\right)\delta \end{pmatrix}. \tag{8}$$

Remark A.1 (*Direct Influence of the Environmental Change in* (S_ε)**).** The fast dynamics of the subpopulation sizes encoded by G (first line of (S_ε)) are independent from the environmental shift, because the latter only directly impacts the dynamics on the local mean traits in (M_ε) (second line). This results in the term $-c$ in the slow dynamics on the average trait Z_ε (second line of (S_ε)).

Remark A.2 (*Initial Conditions: Asymmetrical Equilibrium for Specialists of Habitat 2.*)**.** The initial state of the system $\left(Z^*_{\text{spec}}, N^*_{1,\text{spec}}, N^*_{2,\text{spec}}, \delta^*_{\text{spec}}\right)$ has two particularities that follow its definition in Proposition 4.2 in Dekens (2022). First, it describes a specialist species that is mainly adapted to the native habitat ($Z^*_{\text{spec}} > 0$ is close to its local optimum) and mainly inhabits this habitat ($N^*_{2,\text{spec}}$ is much larger than $N^*_{1,\text{spec}}$, which means that $\rho^*_{\text{spec}} > 1$). Second, the initial specialist population hereby described is at equilibrium under a stable environment ($c = 0$). This means that it both cancels the fast dynamics of the subpopulation sizes represented by the function G in (S_ε):

$$G\left(Z^*_{\text{spec}}, N^*_{1,\text{spec}}, N^*_{2,\text{spec}}, \delta^*_{\text{spec}}\right) = 0_{\mathbb{R}^3},$$

and the slow dynamics of the average trait Z_ε (right-hand side of the second equation of (S_ε) at the main order when $c = 0$):

$$\frac{m}{2g}\delta^*_{\text{spec}}\left(\rho^*_{\text{spec}} - \frac{1}{\rho^*_{\text{spec}}}\right) - Z^*_{\text{spec}} = \frac{\rho^*_{\text{spec}} - \frac{1}{\rho^*_{\text{spec}}}}{\rho^*_{\text{spec}} + \frac{1}{\rho^*_{\text{spec}}}} - Z^*_{\text{spec}} = 0. \tag{9}$$

The two previous remarks justifies the separation of time scales, as it relies on the local stability of the fast dynamics, which is the same as in Dekens (2022). Therefore, the time scales between demographic dynamics and trait dynamics can be separated when $\varepsilon \to 0$, as stated by Theorem 3.1 of Dekens (2022), whereby the solutions of (S_ε) converge to the solutions $\left(Z(t), N_1(t), N_2(t), \delta(t)\right)$ of the following system:

$$\begin{cases} G(Z(t), N_1(t), N_2(t), \delta(t)) = 0_{\mathbb{R}^3}, \\ \frac{dZ}{dt} = -c + 2g\left[\frac{m}{2g}\delta(t)\left(\rho(t) - \frac{1}{\rho(t)}\right) - Z(t)\right] \\ (Z(0), N_1(0), N_2(0), \delta(0)) = \left(Z^*_{\text{spec}}, N^*_{1,\text{spec}}, N^*_{2,\text{spec}}, \delta^*_{\text{spec}}\right). \end{cases} \tag{S}$$

Note also that the (slow) timescale for the differential equation on the second line of (S_ε) corresponds precisely to the timescale of how selection shifts the metapopulation mean trait Z_ε. In other words, it is precisely the one where the variance in trait in the metapopulation scales to 1. There are two advantages to (S). First, due to the separation of time scales, the demographical dynamics are instantly resolved for any current value of the average trait in the metapopulation $Z(t)$ (as the first line of (S) is an algebraic equation, not a differential one). Second, the metapopulation is monomorphic, which is revealed by the fact that the dynamical variable $Z(t)$ is the average trait in the metapopulation. This is because the gene flow by migration occurs at the fast time scale, as opposed to the shift of local mean traits due to selection. As a result, the two local mean traits merge on the fast time scale into $Z(t)$, which then moves slowly according to the gradient of selection represented by the right-hand side of the second line of (S). More precisely, the latter pushes towards an integrative optimum $\frac{m}{2g}\delta(t)\left(\rho(t) - \frac{1}{\rho(t)}\right)$ resulting from the demographical balance of the system.

Moreover, the analysis done in Dekens (2022) allows to further simplify the system (S). It shows that the population can actually be fully described by its average mean trait Z and the ratio between subpopulations sizes $\rho = \frac{N_2}{N_1}$. Their dynamics are given by (S_0).

Appendix B. Antisymmetry of the selection gradient under a stable environment $\mathcal{F}^{c=0}$

Recall that the selection gradient under a stable environment is defined as

$$\mathcal{F}^{c=0}(Z) := 2g\left[\frac{\rho(Z) - \frac{1}{\rho(Z)}}{\rho(Z) + \frac{1}{\rho(Z)}} - Z\right],$$

where the ratio of subpopulation sizes at (ecological) equilibrium $\rho(Z)$ (when the metapopulation mean trait is Z) is defined as the largest root of $P_Z(X) = X^3 - f_1(Z)X^2 + f_2(Z)X - 1$, where $f_1(Z) = 1 + \frac{g}{m}(Z+1)^2 - \frac{1}{m}$ and $f_2(Z) = 1 + \frac{g}{m}(Z-1)^2 - \frac{1}{m}$. f_1 and f_2 are similar because of the symmetry in the environment: the migration rate is the same for both directions and the selection strength parameter g is the same in both habitats.

One can compute that $f_1(-Z) = 1 + \frac{g}{m}(-Z+1)^2 - \frac{1}{m} = f_2(Z)$. This implies in turn that $P_{-Z}(1/X) = -X^3 P_Z(X)$. As $\rho(Z)$ is defined as the largest root of P_Z, we thus obtained that $\rho(-Z) = \frac{1}{\rho(Z)}$. Combining the latter with the fact that $f : \mathbb{R}_+^*, \to \mathbb{R}, x \mapsto \frac{x - \frac{1}{x}}{x + \frac{1}{x}}$ satisfies $f\left(\frac{1}{x}\right) = -f(x)$ results in $\mathcal{F}^{c=0}$ being antisymmetric.

Appendix C. Metapopulation size's initial increase

In this appendix, I show that $\frac{d(N_1+N_2)}{dt}(t=0) > 0$, which implies that, when the environment starts changing, the metapopulation size increases. The intuition is that at the start of environmental change, the initially deserted refugium becomes more suited to support the species as the native habitat becomes less suited. However, because of the quadratic selections functions and the sign of $Z^*_{\text{spec}} > 0$, the gain of quality in the refugium is greater (with an initial selection gradient of $2g(Z^*_{\text{spec}} + 1)$ that the loss of quality in the native one (with an initial selection gradient of $-2g(Z^*_{\text{spec}} - 1)$).

Proof. Following the notations of Lemma 1 in Dekens (2022), I define $\rho := \frac{N_2}{N_1}$ the ratio of subpopulation sizes and the following polynomial form: $P_Z(X) := X^3 - f_1(Z)X^2 + f_2(Z)X - 1$, with $f_1(Z) := 1 + \frac{g}{m}(Z+1)^2 - \frac{1}{m}$ and $f_2(Z) := 1 + \frac{g}{m}(Z-1)^2 - \frac{1}{m}$.

From Lemma 1 in Dekens (2022), for $Z \in \mathbb{R}$, the triplet $(N_1, N_2, \delta) \in \left(\mathbb{R}_+^*\right)^2 \times \mathbb{R}$ is a fast equilibrium at the level Z (ie. $G(Z, N_1, N_2, \delta) = 0$) if and only if $P_Z(\rho) = 0$ and $\rho > \max(0, f_1(Z))$. If this is the case, (N_1, N_2, δ) is given by $\left(m(\rho - f_1(Z)), m\left(\frac{1}{\rho} - f_2(Z)\right), \frac{2g}{m\left(\rho + \frac{1}{\rho}\right)}\right)$.

The system (S) is therefore equivalent to

$$\begin{cases} P_{Z(t)}(\rho(t)) = 0, \quad \rho(t) > \max(0, f_1(Z(t))), \\ \frac{dZ(t)}{dt} = -c + 2g\left[\frac{\rho(t)^2 - 1}{\rho(t)^2 + 1} - Z(t)\right], \\ (Z(0), \rho(0)) = \left(Z^*_{\text{spec}}, \frac{N^*_{2,\text{spec}}}{N^*_{1,\text{spec}}}\right). \end{cases} \tag{10}$$

Hence, the derivative of the metapopulation size à time $t = 0$ is given by

$$\begin{aligned} \frac{d\left[N_1 + N_2\right]}{dt}(t=0) &= \frac{d\left[N_1 + N_2\right]}{dZ}(Z^*_{\text{spec}}) \times \frac{dZ}{dt}(t=0) \\ &= -c \times \frac{d\left[N_1 + N_2\right]}{dZ}(Z^*_{\text{spec}}), \end{aligned}$$

thanks to (9).

It is therefore sufficient to show that $\frac{d[N_1+N_2]}{dZ}(Z^*_{\text{spec}}) < 0$. Recalling that (N_1, N_2) is given by $\left(m(\rho - f_1(Z)), m(\frac{1}{\rho} - f_2(Z))\right)$ where $P_Z(\rho) = 0$, we deduce that:

$$\begin{aligned} \frac{d\left[N_1 + N_2\right]}{dZ}(Z) &= m\left(\frac{d\left[\rho + \frac{1}{\rho}\right]}{dZ}(Z) - f_1'(Z) - f_2'(Z)\right) \\ &= m\left(\rho'(Z)\left(1 - \frac{1}{\rho(Z)^2}\right) - f_1'(Z) - f_2'(Z)\right) \\ &= m\left(-\frac{\partial_Z P_Z(\rho(Z))}{P'_Z(\rho(Z))}\left(1 - \frac{1}{\rho(Z)^2}\right) - f_1'(Z) - f_2'(Z)\right), \end{aligned}$$

where I used that $\rho'(Z) \times P'_Z(\rho(Z)) + \partial_Z P_Z(\rho) = 0$ (since $P_Z(\rho(Z)) = 0$) and that $P'_Z(\rho(Z)) > 0$, since $\rho(Z)$ is the largest root of P_Z (and has multiplicity one).

Moreover, because $P_Z(X) = X^3 - f_1(Z)X^2 + f_2(Z)X - 1$ with $f_1(Z) := 1 + \frac{g}{m}(Z+1)^2 - \frac{1}{m}$ and $f_2(Z) := 1 + \frac{g}{m}(Z-1)^2 - \frac{1}{m}$, we obtain that

$$\begin{aligned} \frac{d\left[N_1 + N_2\right]}{dZ}(Z) &= m\left(\frac{f_1'(Z)\rho(Z)^2 - f_2'(Z)\rho(Z)}{P'_Z(\rho(Z))}\left(1 - \frac{1}{\rho(Z)^2}\right) - f_1'(Z) - f_2'(Z)\right) \\ &= \frac{2g(Z+1)\rho(Z)^2 - 2g(Z-1)\rho(Z)}{P'_Z(\rho(Z))}\left(1 - \frac{1}{\rho(Z)^2}\right) - 4gZ. \end{aligned}$$

Since the computation is performed at $Z = Z^*_{\text{spec}}$ that satisfies $Z^*_{\text{spec}} = \frac{\rho^2(Z^*_{\text{spec}}) - 1}{\rho^2(Z^*_{\text{spec}}) + 1}$, we obtain that

$$\begin{aligned} \frac{d\left[N_1 + N_2\right]}{dZ}(Z^*_{\text{spec}}) &= 4g\left[\frac{\frac{\rho^4(Z^*_{\text{spec}})}{\rho^2(Z^*_{\text{spec}})+1} + \frac{\rho(Z)}{\rho^2(Z^*_{\text{spec}})+1}}{P'_{Z^*_{\text{spec}}}(\rho(Z^*_{\text{spec}}))}\left(\frac{\rho^2(Z^*_{\text{spec}}) - 1}{\rho^2(Z^*_{\text{spec}})}\right) - Z^*_{\text{spec}}\right] \\ &= 4gZ^*_{\text{spec}}\left[\frac{\rho^3(Z^*_{\text{spec}}) + 1}{P'_{Z^*_{\text{spec}}}(\rho(Z^*_{\text{spec}}))\rho(Z^*_{\text{spec}})} - 1\right] \\ &= \frac{4gZ^*_{\text{spec}}}{P'_{Z^*_{\text{spec}}}(\rho(Z^*_{\text{spec}}))\rho(Z^*_{\text{spec}})} \\ &\quad \times \left[\rho^3(Z^*_{\text{spec}}) + 1 - P'_{Z^*_{\text{spec}}}(\rho(Z^*_{\text{spec}}))\rho(Z^*_{\text{spec}})\right]. \end{aligned}$$

Since $Z^*_{\text{spec}} > 0$ by hypothesis, that $\rho\left(Z^*_{\text{spec}}\right) = \frac{N_2\left(Z^*_{\text{spec}}\right)}{N_1\left(Z^*_{\text{spec}}\right)} > 0$ is the largest root of $P_{Z^*_{\text{spec}}}$ with multiplicity one (see lemma 2 of Dekens (2022)) and that therefore $P'_{Z^*_{\text{spec}}}(\rho(Z^*_{\text{spec}})) > 0$, it is sufficient to determine the sign of the term within brackets to conclude:

$$\begin{aligned} &\rho^3\left(Z^*_{\text{spec}}\right) + 1 - P'_{Z^*_{\text{spec}}}(\rho(Z^*_{\text{spec}}))\rho\left(Z^*_{\text{spec}}\right) \\ &\quad = \rho^3\left(Z^*_{\text{spec}}\right) + 1 - 3\rho^3\left(Z^*_{\text{spec}}\right) + 2f_1\left(Z^*_{\text{spec}}\right)\rho^2\left(Z^*_{\text{spec}}\right) \\ &\qquad\qquad - f_2\left(Z^*_{\text{spec}}\right)\rho\left(Z^*_{\text{spec}}\right) \\ &\quad = -\rho^3\left(Z^*_{\text{spec}}\right) + f_1\left(Z^*_{\text{spec}}\right)\rho^2 - P_{Z^*_{\text{spec}}}\left(\rho\left(Z^*_{\text{spec}}\right)\right) \\ &\quad = -\rho^2\left(Z^*_{\text{spec}}\right)\left(\rho - f_1\left(Z^*_{\text{spec}}\right)\right) \\ &\quad = -\rho^2\left(Z^*_{\text{spec}}\right)\frac{N_1\left(Z^*_{\text{spec}}\right)}{m} < 0. \end{aligned}$$

Hence the result. □

Appendix D. Derivation of $c_{\text{death valley}}$ and $c_{\text{death plain}}$

Explicit analytical expressions for $c_{\text{death valley}}$ and $c_{\text{death plain}}$ are available in the parameter range of interest ($[1 + 2m < 5g] \cap [m^2 > 4g(m-1)]$). One can compute that:

$$\boxed{c_{\text{death plain}} = 2gZ_{\text{death plain}}\left(\frac{2}{Z^2_{\text{death plain}} + 1 + \frac{m-1}{g}} - 1\right)},$$

with

$$Z_{\text{death plain}} = -\sqrt{\frac{(g+1-m)}{g} + \sqrt{\frac{1}{g^2}\left[m^2 - 4g(m-1)\right]}} < 0.$$

Similarly, when $g > 1$:

$$\boxed{c_{\text{death valley}} = 2gZ_{\text{death valley}}\left(\frac{2}{Z^2_{\text{death valley}} + 1 + \frac{m-1}{g}} - 1\right)},$$

with

$$Z_{\text{death valley}} = \sqrt{\frac{(g+1-m)}{g} - \sqrt{\frac{1}{g^2}\left[m^2 - 4g(m-1)\right]}}.$$

Proof. At a dominant trait Z^*, the fast equilibria are defined by $G(Z^*, \bar{Y}^*) = 0$, which is solved by (Lemma 1, Section 3.2 of Dekens (2022))

$$(N_1^*, N_2^*, \delta^*) = \left(m[\rho(Z^*) - f_1(Z^*)],\, m\,\rho(Z^*)\,[\rho(Z^*) - f_1(Z^*)],\, \frac{2g}{m\left(\rho(Z^*) + \frac{1}{\rho(Z^*)}\right)} \right), \tag{11}$$

where $\rho(Z^*)$ is the largest (positive root) of the cubic polynomial

$$P_{Z^*}(X) = X^3 - f_1(Z^*)X^2 + f_2(Z^*)X - 1,$$

and

$$f_1(Z^*) = 1 + \frac{g}{m}(Z^* + 1)^2 - \frac{1}{m}, \quad f_2(Z^*) = 1 + \frac{g}{m}(Z^* - 1)^2 - \frac{1}{m}.$$

(11) implies that the subpopulations sizes N_1^* and N_2^* are positive if and only if $f_1(Z^*) < \rho(Z^*)$. Therefore, the limit of viability occurs for Z^* such that $f_1(Z^*) = \rho(Z^*)$. As $\rho(Z^*)$ is the largest root of P_{Z^*}, the latter leads to $0 = P_{Z^*}(f_1(Z^*)) = f_1(Z^*)f_2(Z^*) - 1$, whose roots are $\pm Z_{\text{death plain}}$ and $\pm Z_{\text{death valley}}$. Consequently, the lowest limit of viability occurs at $Z^* = Z_{\text{death plain}} < 0$. The corresponding critical speed over which the population goes extinct reads (renaming $Z_{\text{death plain}}$ as Z_{DP} for the computation)

$$\begin{aligned}
c_{\text{death plain}} &= \mathcal{F}^{c=0}(Z_{DP}) = 2g\left(\frac{\rho(Z_{DP}) - \frac{1}{\rho(Z_{DP})}}{\rho(Z_{DP}) + \frac{1}{\rho(Z_{DP})}} - Z_{DP}\right) \\
&= 2g\left(\frac{f_1(Z_{DP}) - \frac{1}{f_1(Z_{DP})}}{f_1(Z_{DP}) + \frac{1}{f_1(Z_{DP})}} - Z_{DP}\right) \\
&= 2g\left(\frac{f_1(Z_{DP}) - f_2(Z_{DP})}{f_1(Z_{DP}) + f_2(Z_{DP})} - Z_{DP}\right) \\
&= 2g\left(\frac{4gZ_{DP}}{2m - 2 + 2g\left(Z_{DP}^2 + 1\right)} - Z_{DP}\right) \\
&= 2gZ_{DP}\left(\frac{2}{Z_{DP}^2 + 1 + \frac{m-1}{g}} - 1\right).
\end{aligned}$$

The same applies to $c_{\text{death valley}}$ and $Z_{\text{death valley}}$. □

Appendix E. Proof that $c_{\text{death valley}} < c_{\text{death plain}}$ for all $g > 1$

Suppose that $g > 1$ in addition to the parameter range of interest ($[1 + 2m < 5g] \cap [m^2 > 4g(m-1)]$). I rename here $Z_{\text{death plain}}$ and $Z_{\text{death valley}}$ as Z_{DP} and Z_{DV} respectively, for the length of this proof. I recall that the limit traits for the viability of the population $Z_{DV} > 0 > Z_{DP}$ are defined by their squares being the two real roots of the polynomial $X^2 - SX + P$, with $S = 2\left(1 + \frac{1-m}{g}\right) < 4$ and $P = \left(1 - \frac{1}{g}\right)\left(1 + \frac{2m-1}{g}\right)$ (in the considered parameter range, Proposition 3.2 in Dekens (2022) ensures that the discriminant $S^2 - 4P$ is positive). Moreover, standard algebra implies that $S = Z_{DV}^2 + Z_{DP}^2 > 0$ and $P = Z_{DV}^2 Z_{DP}^2 > 0$. For the sake of clarity, I gather all the inequalities that will be used in the rest of the proof.

$$4 > S = Z_{DV}^2 + Z_{DP}^2 > 0, \quad P = Z_{DV}^2 Z_{DP}^2 > 0, \quad S^2 > 4P, \quad Z_{DV} > 0 > Z_{DP}.$$

Using the expression of $c_{\text{death plain}}$ and $c_{\text{death valley}}$ derived in Appendix D, one can compute (defining $a = 2 - \frac{S}{2} = 1 + \frac{m-1}{g} > 0$ and recalling that $\sqrt{P} = -Z_{DP}Z_{DV}$):

$$\begin{aligned}
\frac{c_{DP} - c_{DV}}{2g} &= Z_{DV} - Z_{DP} + \frac{2Z_{DP}}{Z_{DP}^2 + a} - \frac{2Z_{DV}}{Z_{DV}^2 + a} \\
&= \frac{(Z_{DV} - Z_{DP})(Z_{DV}^2 + a)(Z_{DP}^2 + a) + 2Z_{DP}(Z_{DV}^2 + a) - 2Z_{DV}(Z_{DP}^2 + a)}{(Z_{DV}^2 + a)(Z_{DP}^2 + a)} \\
&= \frac{Z_{DV} - Z_{DP}}{(Z_{DV}^2 + a)(Z_{DP}^2 + a)}\left[(Z_{DV}^2 + a)(Z_{DP}^2 + a) - 2\sqrt{P} - 2a\right] \\
&= \frac{Z_{DV} - Z_{DP}}{(Z_{DV}^2 + a)(Z_{DP}^2 + a)}\left[P + a^2 + Sa - 2\sqrt{P} - 2a\right] \\
&= \frac{Z_{DV} - Z_{DP}}{(Z_{DV}^2 + a)(Z_{DP}^2 + a)}\left[\left(2 - \frac{S}{2}\right)\frac{S}{2} - (2 - \sqrt{P})\sqrt{P}\right].
\end{aligned} \tag{12}$$

Since $Z_{DV} > 0 > Z_{DP}$, $c_{DP} - c_{DV}$ has the sign of $\left[\left(2 - \frac{S}{2}\right)\frac{S}{2} - (2 - \sqrt{P})\sqrt{P}\right]$. Defining the function $f : x \mapsto x(2-x)$, it remains to show that $f\left(\frac{S}{2}\right) > f(\sqrt{P})$.

However, on the one hand, from the inequalities above, $\sqrt{P} < \frac{S}{2}$. On the other hand, from the expression of P and S, one can compute

$$\begin{aligned}
P &= \left(1 - \frac{1}{g}\right)\left(1 + \frac{2m-1}{g}\right) \\
&= \left(1 + \frac{m-1}{g} - \frac{m}{g}\right)\left(1 + \frac{m-1}{g} + \frac{m}{g}\right) \\
&= \left(1 + \frac{m-1}{g}\right)^2 - \frac{m^2}{g^2} \\
&< \left(1 + \frac{m-1}{g}\right)^2 = \left(2 - \frac{S}{2}\right)^2.
\end{aligned} \tag{13}$$

As $0 < S < 4$, we obtain that $\sqrt{P} < \min\left(\frac{S}{2}, 2 - \frac{S}{2}\right)$. Hence, since f is strictly increasing on $[0,1]$, that either $\frac{S}{2} \leq 1$ or $2 - \frac{S}{2} \leq 1$, and that $f\left(\frac{S}{2}\right) = f\left(2 - \frac{S}{2}\right)$, we deduce that $f\left(\sqrt{P}\right) < f\left(\frac{S}{2}\right)$, which concludes the proof.

Appendix F. Proof that $c_{\text{death plain}} - c_{\text{death valley}} \to 0$ when $g \to +\infty$ ($m \leq 1$)

Let me fix $m \leq 1$. In this case, the parameter range that I consider throughout the study ($[1 + 2m < 5g] \cap [m^2 > 4g(m-1)]$) contains the half-line $g \geq 1$. In this paragraph, I prove that $c_{\text{death plain}} - c_{\text{death valley}}$ vanishes when $g \to +\infty$.

From the computation displayed in (12), we have

$$c_{DP} - c_{DV} = 2g \times \frac{Z_{DV} - Z_{DP}}{(Z_{DV}^2 + a)(Z_{DP}^2 + a)}\left[P + a^2 + Sa - 2\sqrt{P} - 2a\right], \tag{14}$$

where $a = 1 + \frac{m-1}{g}$, $P = \left(1 + \frac{m-1}{g}\right)^2 - \frac{m^2}{g^2}$ (see Eq. (13)) and $S = 2\left(1 + \frac{1-m}{g}\right)$.

Moreover, from the expressions of Z_{DV} in (2) and Z_{DP} in (4), one can deduce the following limits: $Z_{DV} \underset{g\to+\infty}{\longrightarrow} 1$ and $Z_{DP} \underset{g\to+\infty}{\longrightarrow} -1$. Therefore, as $a \underset{g\to+\infty}{\longrightarrow} 1$, we obtain that:

$$c_{DP} - c_{DV} \sim g \times \left[P + a^2 + Sa - 2\sqrt{P} - 2a\right], \tag{15}$$

Let us show that the sum within brackets in the r.h.s of Eq. (15) is $\mathcal{O}\left(\frac{1}{g^2}\right)$ when $g \to +\infty$. To that aim, one can compute the following estimations:

$$\begin{aligned}
P &= 1 + \frac{2(m-1)}{g} + \mathcal{O}\left(\frac{1}{g^2}\right), \\
a^2 &= 1 + \frac{2(m-1)}{g} + \mathcal{O}\left(\frac{1}{g^2}\right), \\
Sa &= 2 + \mathcal{O}\left(\frac{1}{g^2}\right), \\
-2\sqrt{P} &= -2 - \frac{2(m-1)}{g} + \mathcal{O}\left(\frac{1}{g^2}\right), \\
-2a &= -2 - \frac{2(m-1)}{g}.
\end{aligned} \tag{16}$$

Summing the different estimations of Eq. (16) in Eq. (15) finally yields that

$$c_{DP} - c_{DV} = \underset{g\to+\infty}{\mathcal{O}}\left(\frac{1}{g}\right),$$

which concludes.

Appendix G. Cost of dispersal: behaviour of $Z_{\text{death plain}}$ and $c_{\text{death plain}}$ with respect to the migration rate m

In this appendix, I will abbreviate $Z_{\text{death plain}}$ and $c_{\text{death plain}}$ as Z_{DP} and c_{DP}. Let $g > 0$ be fixed throughout this appendix. All the following computations are done for $m > 0$ such that $[1 + 2m < 5g] \cap [m^2 > 4g(m-1)]$.

Z_{DP} increases with respect to the migration rate m. Let me first recall the expression of Z_{DP} from (4), denoted here as a function of m for the purpose of this appendix:

$$Z_{DP}(m) = -\sqrt{\frac{g+1-m}{m} + \sqrt{\frac{m^2-4g(m-1)}{g^2}}} < 0.$$

Next, one can differentiate to find:

$$\frac{\partial Z_{DP}}{\partial m} = -\frac{2\sqrt{m^2-4g(m-1)} + 4\ g - 2m}{4g Z_{DP}(m)\sqrt{m^2-4g(m-1)}}.$$

Let me first consider the case $g < 1$. In that case, we deduce that $m \le \frac{5\ g-1}{2} \le \frac{5\ g-g}{2} = 2g$. Therefore, as $Z_{DP}(m)$ is negative, the above quantity $\partial_m Z_{DP}$ is positive.

Let me now consider the case $g \ge 1$. Then, from Remark 4.4 of Dekens (2022), the condition $[1 + 2m < 5g] \cap [m^2 > 4g(m-1)]$ is equivalent to $m < 2g\left(1 - \sqrt{1 - \frac{1}{g}}\right)$, which is in turn lower than $2g$. By the same argument as above, I obtain that $\partial_m Z_{DP}$ is positive.

Therefore, Z_{DP} increases with respect to the migration rate m.

c_{DP} decreases with respect to the migration rate m. Let me first recall the expression of c_{DP} from (5). To do so, it is practical to first define the following function:

$$f : (Z, m) \mapsto 2gZ\left(\frac{2}{Z^2 + 1 + \frac{m-1}{g}} - 1\right),$$

so that we have:

$$c_{DP}(m) = f\left(Z_{DP}(m), m\right).$$

From the latter, one can differentiate and compute (omitting the dependency of the variables with the migration rate after the first line in the sake of clarity)

$$\begin{aligned}\frac{\partial c_{DP}}{\partial m}(m) &= \frac{\partial f}{\partial m}\left(Z_{DP}(m), m\right) + \frac{\partial Z_{DP}}{\partial m}(m)\frac{\partial f}{\partial Z}\left(Z_{DP}(m), m\right)\\ &= \frac{-4Z_{DP}}{\left(Z_{DP}^2 + 1 + \frac{m-1}{g}\right)^2} + \frac{\partial Z_{DP}}{\partial m}\left(\frac{c_{DP}}{Z_{DP}} - \frac{8gZ_{DP}^2}{\left(Z_{DP}^2 + 1 + \frac{m-1}{g}\right)^2}\right)\\ &= \frac{c_{DP}}{Z_{DP}}\frac{\partial Z_{DP}}{\partial m} - \frac{4Z_{DP}}{\left(Z_{DP}^2 + 1 + \frac{m-1}{g}\right)^2}\left(1 + 2gZ_{DP}\frac{\partial Z_{DP}}{\partial m}\right).\end{aligned}$$

The first term of the l.h.s is negative, since $c_{DP} > 0$, $Z_{DP} < 0$ and $\frac{\partial Z_{DP}}{\partial m} \ge 0$ (from the previous paragraph). Thus, it suffices to show that the second term of the l.h.s is also negative, ie. that $1 + 2gZ_{DP}\frac{\partial Z_{DP}}{\partial m} \le 0$. To do so, one can use the derivation of $\frac{\partial Z_{DP}}{\partial m}$ in the last paragraph to deduce that:

$$1 + 2gZ_{DP}\frac{\partial Z_{DP}}{\partial m} \le 0 \iff \frac{m-2g}{\sqrt{m^2-4g(m-1)}} < 0.$$

Using the same arguments as in the last paragraph showing that $m \le 2g$ in the considered parameter range concludes the proof and shows that c_{DP} is decreasing with respect to the migration rate m.

Appendix H. Limits of $c_{\text{death plain}}$ and $c_{\text{death valley}}$ as $m \to 0$

In this appendix, I will abbreviate $Z_{\text{death plain}}$ and $Z_{\text{death valley}}$ as Z_{DP} and Z_{DV} and $c_{\text{death plain}}$ and $c_{\text{death valley}}$ as c_{DP} and c_{DV}.

From the expressions of Z_{DP} and Z_{DV} derived in Appendix D, one can compute that

$$\begin{aligned}Z_{DP} &= -\sqrt{\frac{(g+1-m)}{g} + \sqrt{\frac{1}{g^2}\left[m^2 - 4g(m-1)\right]}}\\ &\xrightarrow[m\to0]{} -\sqrt{1 + \frac{1}{g} + \frac{2}{\sqrt{g}}} = -\left(1 + \frac{1}{\sqrt{g}}\right).\end{aligned}$$

Similarly, when $g \ge 1$, one can compute that

$$\begin{aligned}Z_{DV} &= \sqrt{\frac{(g+1-m)}{g} - \sqrt{\frac{1}{g^2}\left[m^2 - 4g(m-1)\right]}}\\ &\xrightarrow[m\to0]{} \sqrt{1 + \frac{1}{g} - \frac{2}{\sqrt{g}}} = 1 - \frac{1}{\sqrt{g}}.\end{aligned}$$

Now using the expressions of c_{DP} and c_{DV} derived in Appendix D along the previously derived results leads to

$$c_{DP} \xrightarrow[m\to0]{} -2g\left(1 + \frac{1}{\sqrt{g}}\right)\left(\frac{1}{1 + \frac{1}{\sqrt{g}}} - 1\right) = 2\sqrt{g}.$$

Similarly, when $g \ge 1$, one computes that

$$c_{DV} \xrightarrow[m\to0]{} 2g\left(1 - \frac{1}{\sqrt{g}}\right)\left(\frac{1}{1 - \frac{1}{\sqrt{g}}} - 1\right) = 2\sqrt{g}.$$

The common limit of c_{DP} and c_{DV} under vanishing migration rate ($m \to 0$) coincides with the critical speed of environmental change in single-habitat models (see for example (Kopp and Matuszewski, 2014) - recall that the population's trait variance has been here rescaled to 1 in the considered timescale and that the width of the fitness function is $\frac{1}{2g}$).

Appendix I. Monotony of $\rho(z)$

Let $Z \in [-1, 1]$ be such that $\rho(Z)$ is the only positive root of $P_Z(X) = X^3 - f_1(Z)X^2 + f_2(Z)X - 1$ greater than $f_1(Z)$, so that the viability of the metapopulation is ensured (see Dekens (2022) for details). From $P_Z(\rho(Z)) = 0$, we get

$$\rho'(Z) = \rho(Z)\frac{f_1'(Z)\rho(Z) - f_2'(Z)}{P_Z'(\rho(Z))}. \tag{17}$$

As $\rho(Z) > 0$ is the largest root of P_Z (see Dekens (2022)), $P_Z'(\rho(Z)) > 0$. Therefore, $\rho'(Z)$ has the sign of $f_1'(Z)\rho(Z) - f_2'(Z)$.

Example of monotony: in the case where f_1 is increasing on $[-1, +\infty[$ and f_2 is decreasing on $]-\infty, 1]$ (like in the quadratic case), then ρ is an increasing function of $Z \in [-1, 1]$.

Appendix J. Supplementary figures from stochastic IBS's results

In this appendix, I compare the analytical predictions regarding the equilibrium values of the metapopulation size and mean trait derived in Section 3 with the end results of stochastic individual-based simulations (IBS) meant to provide a stochastic version of the dimensionless system (S_ε). The migration and selection parameters used in the following display are those used in Fig. 5, which are $m = 0.5$, $g = 0.7; 1.1; 1.4; 1.8$.

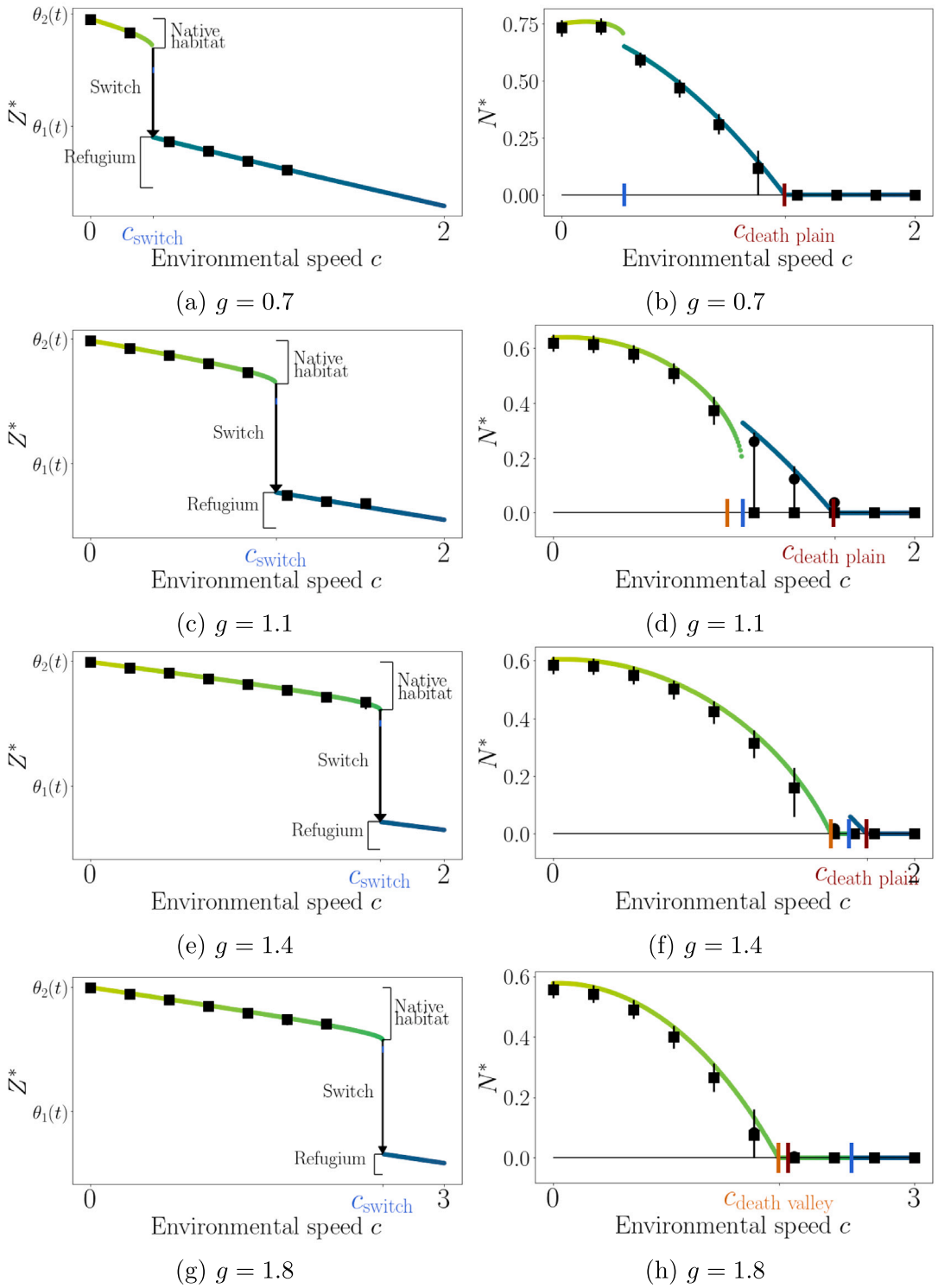

Fig. 7. Same as Fig. 5 with final results of stochastic IBS instead of deterministic numerical resolutions. As in Fig. 5, the coloured curves correspond to the analytical solution of (S_0) (green in the native habitat, blue in the refugium). The black squares represent the median quantities from the IBS and the vertical black lines span the results of 98% of the stochastic trajectories. Moreover, regarding the plots of N^* (right column), the black circles indicate the median metapopulation size across non-extinct populations. Mean traits of extinct populations are ill-defined and thus not displayed.

IBS's design. The IBS are designed as follows. They consider discrete generations (where the same life cycle unfolds before starting the next generation) that are also overlapping (individuals can potentially survive over several generations). For a given selection parameter g, $N_{\text{replicates}}$ replicate simulations are run first for 100 generations of burn-in, and next for a fixed number of generations N_{gen}, which is sufficient to reach an equilibrium. Moreover, each generation spans a small time-step $dt = 10^{-2}$, which rescales every biological rate involved (so that only a few events of birth, death and migration occur during each generation). Consequently, one time unit spans 100 generations. The choice of small time-step generations aims at setting the IBS so that they constitute an accurate stochastic description of the system of

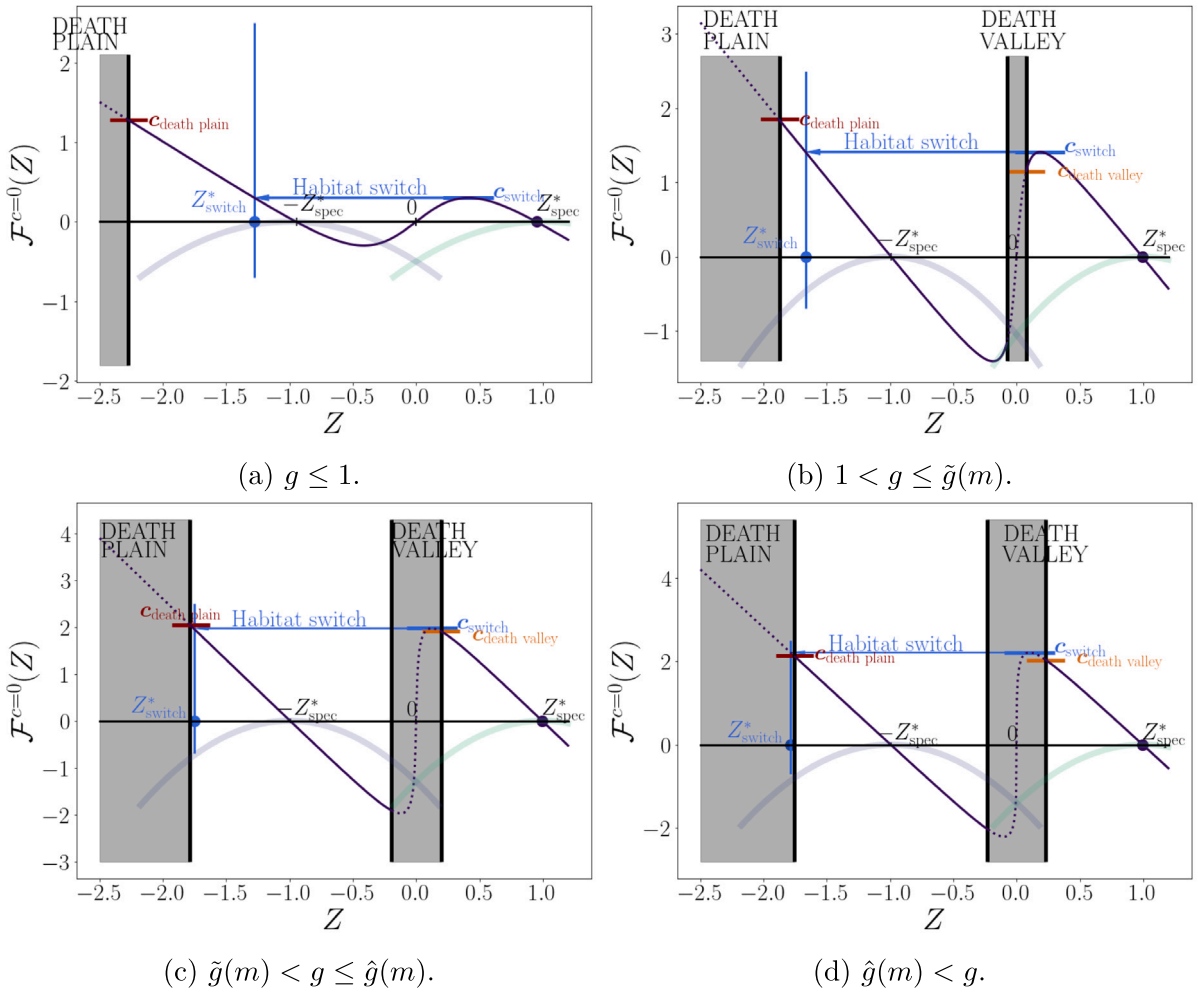

Fig. 8. Same as Fig. 3, but with $m = 0.2$ and $g = 0.5, 1.05, 1.3, 1.4$ (top to bottom, left to right).

differential Eqs. (S_ε), which considers per essence (infinitesimally) small time steps. For $g = 0.7; 1.1; 1.4; 1.8$, $N_{\text{replicates}} = 250; 1000; 1000; 1000$ and $N_{\text{gen}} = 3.5 \times 10^6; 2 \times 10^6; 10^6; 5 \times 10^5$. The large number of replicates meant to ensure that (rare) evolutionary rescue events would be captured in most cases. Notice that the number of replicates for $g = 0.7$ is relatively low (250, which is still quite large), as the analysis predicts that no evolutionary rescue is expected in this case and that cutting the number of replicate simulations speeds up the computational time. Each replicate simulation is run according to the same following scheme:

- Each habitat has the same carrying capacity $K = 10^4$ individuals. Initially, there are $\lfloor N^*_{1,\text{spec}} \times K \rfloor$ individuals in the refugium and $\lfloor N^*_{2,\text{spec}} \times K \rfloor$ individuals in the native habitat, where $N^*_{1,\text{spec}}$ and $N^*_{2,\text{spec}}$ are the rescaled equilibrium subpopulations sizes under stable environment indicated in Proposition 4.2 of Dekens (2022). Their traits are randomly drawn from a Gaussian distribution of mean Z^*_{spec} and with a small variance ε^2, with $\varepsilon^2 = 5 \times 10^{-3}$.
- First, the environment is stable during 100 generations. Next, the environment changes with a speed $\varepsilon^2 c$, meaning that in habitat i and at generation t after the burn-in, the local optimal trait is given by $\theta_i(t) = \theta_i(0) + \varepsilon^2 ct$, with $1 \leq t \leq N_{\text{gen}}$.
- At each generation t, the following life cycle unfolds over a timespan dt:

  1. Reproduction event: in each subpopulation i, a random number of individuals are uniformly sampled across the subpopulation according to a Binomial distribution of mean $N_i(t) \times dt$ (ie. $N_i(t) \times dt$ individuals chosen on average). For each of these individuals, a mate is uniformly chosen at random within the same subpopulation. Their mating produces a single child who is added to the same subpopulation and whose trait is drawn randomly from a Gaussian distribution centred on the mean parental trait and with variance $\frac{\varepsilon^2}{2}$. At the end of the reproduction event, the subpopulation size is $N_i^{\text{post reprod}}(t)$ (which is thus on average equal to $N_i(1 + dt)$).
  2. Selection-density regulation event: in each subpopulation living in habitat i with optimal trait $\theta_i(t)$, each individual faces a selection-density regulation trial, according to its trait z and the current subpopulation size $N_i^{\text{post reprod}}(t)$. Precisely, individuals survive according to independent Bernoulli random variables with parameters given by:

$$\exp\left[-g \times dt \times \left(z - \theta_i(t)\right)^2\right] \times \exp\left[-\frac{dt \times N_i^{\text{post reprod}}(t)}{K}\right].$$

     The first exponential term quantifies the probability of surviving through the trait-dependent selection process for individuals with trait z. The second exponential represents the probability of surviving the density regulation process within a subpopulation of $N_i^{\text{post reprod}}(t)$. Any individual who fails the trial is removed and the subpopulation size at the end of this phase is $N_i^{\text{post sel-regul}}(t)$.

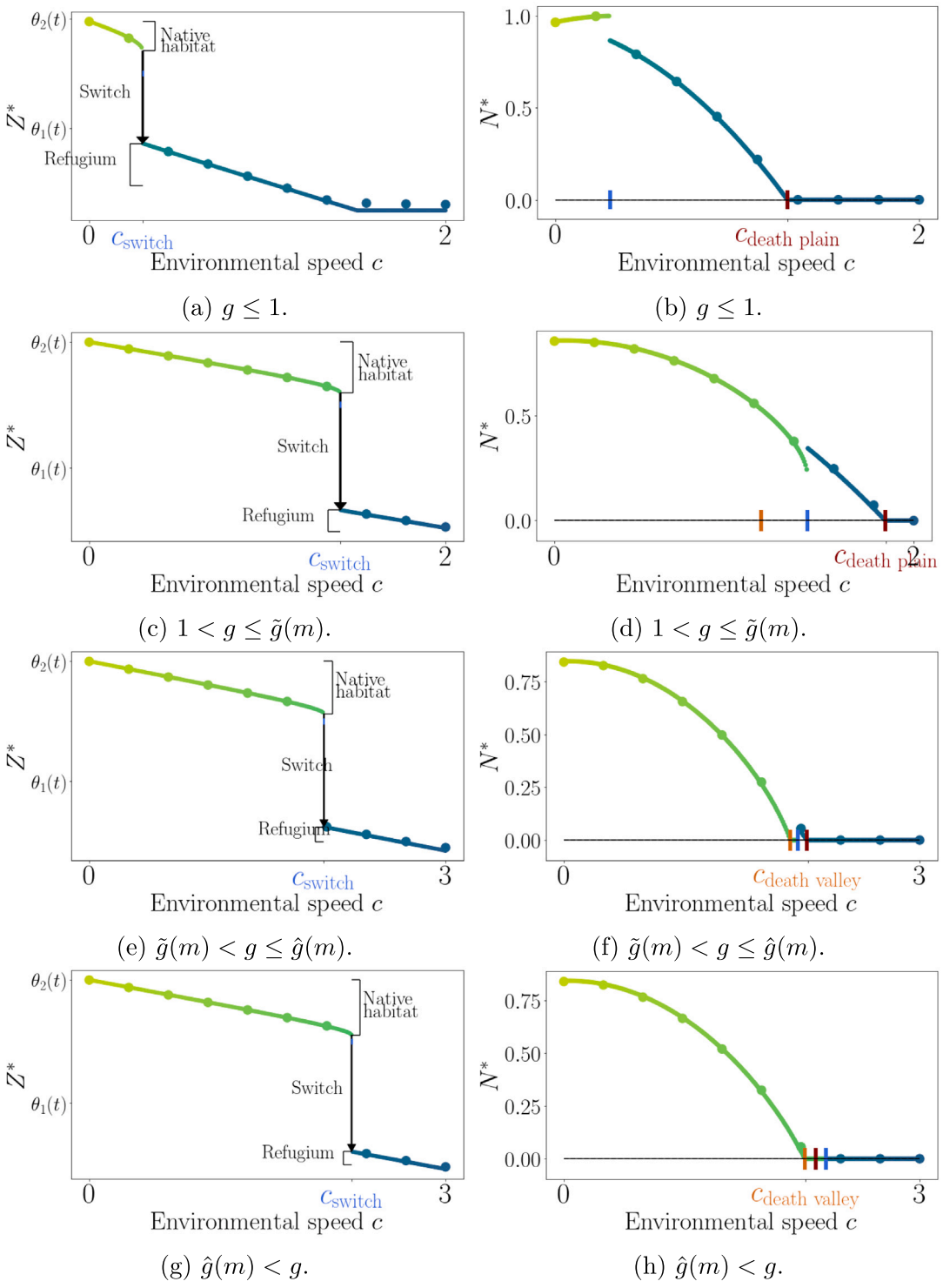

Fig. 9. Same as Fig. 5, but with $m = 0.2$ and $g = 0.5, 1.05, 1.3, 1.4$ (top to bottom).

3. Migration event: in each subpopulation i independently, a random number of migrants is drawn according to a Poisson distribution of parameter $m \times dt \times N_i^{\text{post sel-regul}}(t)$. These migrants are then removed from their current subpopulation and added to the other one.

IBS's results. The comparison between the analytical predictions of the equilibrium variables (Z^* the metapopulation mean trait and N^* the metapopulation size) and the analogous final quantities of the IBS is displayed in Fig. 7. The overall conclusion is that the IBS are in excellent agreement with the predictions, especially for the metapopulation mean trait Z^* conditional on persistence (left column). The same can be said for the metapopulation size, albeit with more variance near extinction (vertical black lines, representing 98% of the trajectories) as expected by random stochastic fluctuations. These have a striking impact when the metapopulation relies on evolutionary rescue, which

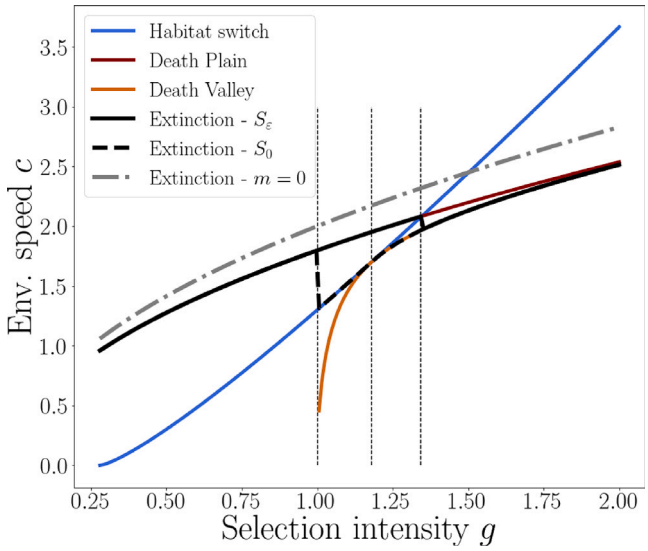

Fig. 10. Same as Fig. 6, but with $m = 0.2$.

is predicted to occur when $g > 1$ (bottom three lines), and is highlighted particularly in Fig. 7(d). Notice that for the 6th, 7th and 8th environmental speeds, the median metapopulation size (black squares) is 0, indicating extinction. However, the variance between replicates can be high and the median metapopulation size of non-extinct populations (black circles) is very close to the analytically predicted metapopulation size. The IBS give some quantitative indications that the probability of rescue is probably less than half and more than $1/N_{\text{replicates}} = 10^{-3}$ (whereas this probability of rescue cannot be quantified from my analysis). Moreover, it shows that when the population does get rescued, its final state is accurately predicted by my analysis.

Appendix K. Supplementary figures with low migration rate $m = 0.2$

See Figs. 7–10.

References

Adams-Hosking, C., McAlpine, C., Rhodes, J.R., Grantham, H.S., Moss, P.T., 2012. Modelling changes in the distribution of the critical food resources of a specialist folivore in response to climate change: Modelling range contractions in koalas and their food resources. Diversity and Distributions (ISSN: 13669516) 18 (9), 847–860. http://dx.doi.org/10.1111/j.1472-4642.2012.00881.x.

Aguilée, R., Raoul, G., Rousset, F., Ronce, O., 2016. Pollen dispersal slows geographical range shift and accelerates ecological niche shift under climate change. Proc. Natl. Acad. Sci. 113 (39), http://dx.doi.org/10.1073/pnas.1607612113 (ISSN 0027-8424, 1091-6490) URL: https://pnas.org/doi/full/10.1073/pnas.1607612113.

Alfaro, M., Berestycki, H., Raoul, G., 2017. The effect of climate shift on a species submitted to dispersion, evolution, growth, and nonlocal competition. SIAM J. Math. Anal. 49 (1), 562–596. http://dx.doi.org/10.1137/16M1075934 (ISSN 0036-1410, 1095-7154).

Barfield, M., Holt, R.D., Gomulkiewicz, R., 2011. Evolution in stage-structured populations. Amer. Nat. 177 (4), 397–409. http://dx.doi.org/10.1086/658903 (ISSN 0003-0147, 1537-5323).

Barton, N.H., Etheridge, A.M., Véber, A., 2017. The infinitesimal model: Definition, derivation, and implications. Theor. Popul. Biol. (ISSN: 00405809) 118, 50–73. http://dx.doi.org/10.1016/j.tpb.2017.06.001.

Berg, M.P., Kiers, E.T., Driessen, G., van der Heijden, M., Kooi, B.W., Kuenen, F., Liefting, M., Verhoef, H.A., Ellers, J., 2010. Adapt or disperse: understanding species persistence in a changing world. Global Change Biol. 16 (2), 587–598. http://dx.doi.org/10.1111/j.1365-2486.2009.02014.x (ISSN 13541013, 13652486).

Botero, G.A., Weissing, F.J., Wright, J., Rubenstein, D.R., 2015. Evolutionary tipping points in the capacity to adapt to environmental change. Proc. Natl. Acad. Sci. 112 (1), 184–189. http://dx.doi.org/10.1073/pnas.1408589111 (ISSN 0027-8424, 1091-6490).

Bourne, E.C., Bocedi, G., Travis, J.M.J., Pakeman, R.J., Brooker, R.W., Schiffers, K., 2014. Between migration load and evolutionary rescue: dispersal, adaptation and the response of spatially structured populations to environmental change. Proc. R. Soc. Lond. [Biol.] 281 (1778), 20132795. http://dx.doi.org/10.1098/rspb.2013.2795 (ISSN 0962-8452, 1471-2954).

Bulmer, M.G., 1971. The effect of selection on genetic variability. Amer. Nat. 105 (943), 201–211.

Bürger, R., 1999. Evolution of genetic variability and the advantage of sex and recombination in changing environments. Genetics (ISSN: 1943-2631) 153 (2), 1055–1069. http://dx.doi.org/10.1093/genetics/153.2.1055.

Bürger, R., 2000. The mathematical theory of selection, recombination, and mutation.

Bürger, R., Lynch, M., 1995. Evolution and extinction in a changing environment: A quantitative-genetic analysis. Evolution 49 (1), 151–163. http://dx.doi.org/10.1111/j.1558-5646.1995.tb05967.x (ISSN 0014-3820, 1558-5646).

Calvez, V., Garnier, J., Patout, F., 2019. Asymptotic analysis of a quantitative genetics model with nonlinear integral operator. J. l'École Polytech. (ISSN: 2270-518X) 6, 537–579. http://dx.doi.org/10.5802/jep.100.

Chaparro-Pedraza, P.C., 2021. Fast environmental change and eco-evolutionary feedbacks can drive regime shifts in ecosystems before tipping points are crossed. Proc. R. Soc. Lond. [Biol.] 288 (1955), 20211192. http://dx.doi.org/10.1098/rspb.2021.1192 (ISSN 0962-8452, 1471-2954).

Chevin, L.-M., Lande, R., Mace, G.M., 2010. Adaptation, plasticity, and extinction in a changing environment: Towards a predictive theory. In: Kingsolver, Joel G. (Ed.), PLoS Biol. (ISSN: 1545-7885) 8 (4), e1000357. http://dx.doi.org/10.1371/journal.pbio.1000357.

Clavel, J., Julliard, R., Devictor, V., 2011. Worldwide decline of specialist species: toward a global functional homogenization? Front. Ecol. Environ. 9 (4), 222–228. http://dx.doi.org/10.1890/080216 (ISSN 1540-9295, 1540-9309).

Corlett, R.T., Tomlinson, K.W., 2020. Climate change and edaphic specialists: Irresistible force meets immovable object? Trends Ecol. Evolut. (ISSN: 01695347) 35 (4), 367–376. http://dx.doi.org/10.1016/j.tree.2019.12.007.

Cotto, O., Ronce, O., 2014. Maladaptation as a source of senescence in habitats variable in space and time: Maladaptation as a source of senescence. Evolution (ISSN: 00143820) 68 (9), 2481–2493. http://dx.doi.org/10.1111/evo.12462.

Cotto, O., Sandell, L., Chevin, L-M, Ronce, O., 2019. Maladaptive shifts in life history in a changing environment. Amer. Nat. 194 (4), 558–573. http://dx.doi.org/10.1086/702716 (ISSN 0003-0147, 1537-5323).

Cotto, O., Wessely, J., Georges, D., Klonner, G., Schmid, M., Dullinger, S., Thuiller, W., Guillaume, F., 2017. A dynamic eco-evolutionary model predicts slow response of alpine plants to climate warming. Nature Commun. (ISSN: 2041-1723) 8 (1), 15399. http://dx.doi.org/10.1038/ncomms15399.

Dakos, V., Matthews, B., Hendry, A.P., Levine, J., Loeuille, N., Norberg, J., Nosil, P., Scheffer, M., De Meester, L., 2019. Ecosystem tipping points in an evolving world. Nat. Ecol. Evol. (ISSN: 2397-334X) 3 (3), 355–362. http://dx.doi.org/10.1038/s41559-019-0797-2.

Damschen, E.I., Harrison, S., Ackerly, D.D., Fernandez-Going, B.M., Anacker, B.L., 2012. Endemic plant communities on special soils: early victims or hardy survivors of climate change?: Special soils, endemics, and climate change. J. Ecol. (ISSN: 00220477) 100 (5), 1122–1130. http://dx.doi.org/10.1111/j.1365-2745.2012.01986.x.

Débarre, F., Ronce, O., Gandon, S., 2013. Quantifying the effects of migration and mutation on adaptation and demography in spatially heterogeneous environments. J. Evol. Biol. (ISSN: 1010061X) 26 (6), 1185–1202. http://dx.doi.org/10.1111/jeb.12132.

Dekens, L., 2022. Evolutionary dynamics of complex traits in sexual populations in a heterogeneous environment: how normal? J. Math. Biol. 84 (3), 15. http://dx.doi.org/10.1007/s00285-021-01712-0 (ISSN 0303-6812, 1432-1416).

Dekens, L., Lavigne, F., 2021. Front propagation of a sexual population with evolution of dispersion: A formal analysis. SIAM J. Appl. Math..

Duputié, A., Massol, F., Chuine, I., Kirkpatrick, M., Ronce, O., 2012. How do genetic correlations affect species range shifts in a changing environment?: Multivariate adaptation and range shifts. Ecol. Lett. (ISSN: 1461023X) 15 (3), 251–259. http://dx.doi.org/10.1111/j.1461-0248.2011.01734.x.

Ehrlén, J., Morris, W.F., 2015. Predicting changes in the distribution and abundance of species under environmental change. In: Buckley, Yvonne (Ed.), Ecol. Lett. 18 (3), 303–314. http://dx.doi.org/10.1111/ele.12410 (ISSN 1461-023X, 1461-0248).

Fisher, R.A., 1919. The correlation between relatives on the supposition of mendelian inheritance. Trans. Royal Soc. Edinb. 52 (2), 399–433. http://dx.doi.org/10.1017/S0080456800012163.

Garnier, J., Cotto, O., Bouin, E., Bourgeron, T., Lepoutre, T., Ronce, O., Calvez, V., 2023. Adaptation of a quantitative trait to a changing environment: New analytical insights on the asexual and infinitesimal sexual models. Theor. Popul. Biol. (ISSN: 00405809) 152, 1–22. http://dx.doi.org/10.1016/j.tpb.2023.04.002.

Hendry, A.P., Day, T., Taylor, E.B., 2001. Population mixing and the adaptive divergence of quantitative traits in discrete populations: A theoretical framework for empirical tests. Evolution (ISSN: 00143820) 55 (3), 459–466. http://dx.doi.org/10.1111/j.0014-3820.2001.tb00780.x.

Hof, A.R., Jansson, R., Nilsson, C., 2012. Future climate change will favour non-specialist mammals in the (sub)arctics. In: Romanuk, Tamara Natasha (Ed.), PLoS One (ISSN: 1932-6203) 7 (12), e52574. http://dx.doi.org/10.1371/journal.pone.0052574.

Hoffmann, A.A., Sgrò, C.M., 2011. Climate change and evolutionary adaptation. Nature 470 (7335), 479–485. http://dx.doi.org/10.1038/nature09670 (ISSN 0028-0836, 1476-4687).

Holt, R.D., Gomulkiewicz, R., Barfield, M., 2003. The phenomenology of niche evolution via quantitative traits in a 'black-hole' sink. Proc. R. Soc. Lond. [Biol.] 270 (1511), 215–224. http://dx.doi.org/10.1098/rspb.2002.2219 (ISSN 0962-8452, 1471-2954).

Kirkpatrick, M., Barton, N.H., 1997. Evolution of a species' range. Amer. Nat. 150 (1), 1–23. http://dx.doi.org/10.1086/286054, PMID: 18811273.

Klausmeier, C.A., Osmond, M.M., Kremer, C.T., Litchman, E., 2020. Ecological limits to evolutionary rescue. Phil. Trans. R. Soc. B 375 (1814), 20190453. http://dx.doi.org/10.1098/rstb.2019.0453 (ISSN 0962-8436, 1471-2970).

Kopp, M., Matuszewski, S., 2014. Rapid evolution of quantitative traits: theoretical perspectives. Evol. Appl. (ISSN: 1752-4571, 1752-4571) 7 (1), 169–191. http://dx.doi.org/10.1111/eva.12127.

Lande, R., Shannon, S., 1996. The role of genetic variation in adaptation and population persistence in a changing environment. Evolution 50 (1), 434–437.

Lavigne, F., 2023. Adaptation of an asexual population with environmental changes. Math. Model. Nat. Phenom. 18, 20. http://dx.doi.org/10.1051/mmnp/2023024 (ISSN 0973-5348, 1760-6101).

Lenoir, J., Gégout, J.C., Marquet, P.A., De Ruffray, P., Brisse, H., 2008. A significant upward shift in plant species optimum elevation during the 20th century. Science 320 (5884), 1768–1771. http://dx.doi.org/10.1126/science.1156831 (ISSN 0036-8075, 1095-9203).

Lynch, M., Lande, R., 1993. Biotic Interactions and Global Change. Sinauer, Sunderland, MA, pp. 234–250,

McLaughlin, B.C., Ackerly, D.D., Klos, P.Z., Natali, J., Dawson, T.E., Thompson, S.E., 2017. Hydrologic refugia, plants, and climate change. Global Change Biol. 23 (8), 2941–2961. http://dx.doi.org/10.1111/gcb.13629 (ISSN 1354-1013, 1365-2486).

McManus, L.C., Tekwa, E.W., Schindler, D.E., Walsworth, T.E., Colton, M.A., Webster, M.M., Essington, T.E., Forrest, D.L., Palumbi, S.R., Mumby, P.J., Pinsky, M.L., 2021. Evolution reverses the effect of network structure on metapopulation persistence. Ecology 102 (7), http://dx.doi.org/10.1002/ecy.3381 (ISSN 0012-9658, 1939-9170) URL: https://onlinelibrary.wiley.com/doi/10.1002/ecy.3381.

Mirrahimi, S., 2017. A Hamilton–Jacobi approach to characterize the evolutionary equilibria in heterogeneous environments. Math. Models Methods Appl. Sci. (ISSN: 0218-2025) 27 (13), 2425–2460. http://dx.doi.org/10.1142/s0218202517500488.

Mirrahimi, S., Gandon, S., 2020. Evolution of specialization in heterogeneous environments: Equilibrium between selection, mutation and migration. Genetics (ISSN: 0016-6731) 214 (2), 479–491. http://dx.doi.org/10.1534/genetics.119.302868.

Mirrahimi, S., Raoul, G., 2013. Dynamics of sexual populations structured by a space variable and a phenotypical trait. Theor. Popul. Biol. (ISSN: 00405809) 84, 87–103. http://dx.doi.org/10.1016/j.tpb.2012.12.003.

Morelli, T.L., Daly, C., Dobrowski, S.Z., Dulen, D.M., Ebersole, J.L., Jackson, S.T., Lundquist, J.D., Millar, C.I., Maher, S.P., Monahan, W.B., Nydick, K.R., Redmond, K.T., Sawyer, S.C., Stock, S., Beissinger, S.R., 2016. Managing climate change refugia for climate adaptation. In: Rebelo, Hugo (Ed.), PLoS One (ISSN: 1932-6203) 11 (8), e0159909. http://dx.doi.org/10.1371/journal.pone.0159909.

Moritz, C., Patton, J.L., Conroy, C.J., Parra, J.L., White, G.C., Beissinger, S.R., 2008. Impact of a century of climate change on small-mammal communities in Yosemite National Park, USA. Science 322 (5899), 261–264. http://dx.doi.org/10.1126/science.1163428 (ISSN 0036-8075, 1095-9203).

Osmond, M.M., Klausmeier, C.A., 2017. An evolutionary tipping point in a changing environment. Evolution (ISSN: 1558-5646) 71 (12), 2930–2941. http://dx.doi.org/10.1111/evo.13374.

Parmesan, C., Ryrholm, N., Stefanescu, C., Hill, J.K., Thomas, C.D., Descimon, H., Huntley, B., Kaila, L., Kullberg, J., Tammaru, T., Tennent, W.J., Thomas, J.A., Warren, M., 1999. Poleward shifts in geographical ranges of butterfly species associated with regional warming. Nature 399 (6736), 579–583. http://dx.doi.org/10.1038/21181 (ISSN 0028-0836, 1476-4687).

Patout, F., 2023. The Cauchy problem for the infinitesimal model in the regime of small variance. Anal. PDE 16 (6), 1289–1350. http://dx.doi.org/10.2140/apde.2023.16.1289 (ISSN 1948-206X, 2157-5045).

Pease, C.M., Lande, R., Bull, J.J., 1989. A model of population growth, dispersal and evolution in a changing environment. Ecology (ISSN: 00129658) 70 (6), 1657–1664. http://dx.doi.org/10.2307/1938100.

Polechová, J., Barton, N., Marion, G., 2009. Species' range: Adaptation in space and time. Amer. Nat. 174 (5), E186–E204. http://dx.doi.org/10.1086/605958 (ISSN 0003-0147, 1537-5323).

Ramirez, A.R., De Guzman, M.E., Dawson, T.E., Ackerly, D.D., 2020. Plant hydraulic traits reveal islands as refugia from worsening drought. In: Hultine, Kevin (Ed.), Conserv. Physiol. (ISSN: 2051-1434) 8 (1), coz115. http://dx.doi.org/10.1093/conphys/coz115.

Raoul, G, 2017. Macroscopic limit from a structured population model to the Kirkpatrick-Barton model. arXiv:1706.04094.

Ronce, O., Kirkpatrick, M., 2001. When sources become sinks: Migrational meltdown in heterogeneous habitats. Evolution (ISSN: 0014-3820) 55 (8), 1520–1531. http://dx.doi.org/10.1111/j.0014-3820.2001.tb00672.x.

Roques, L., Patout, F., Bonnefon, O., Martin, G., 2020. Adaptation in general temporally changing environments. SIAM J. Appl. Math. 80 (6), 2420–2447. http://dx.doi.org/10.1137/20M1322893.

Thompson, P.L., Fronhofer, E.A., 2019. The conflict between adaptation and dispersal for maintaining biodiversity in changing environments. Proc. Natl. Acad. Sci. 116 (42), 21061–21067. http://dx.doi.org/10.1073/pnas.1911796116 (ISSN 0027-8424, 1091-6490).

Tilman, D., May, R.M., Lehman, C.L., Nowak, M.M., 1994. Habitat destruction and the extinction debt. Nature 371, 65–66.

Turelli, M., Barton, N.H., 1990. Dynamics of polygenic characters under selection. Theor. Popul. Biol. (ISSN: 00405809) 38 (1), 1–57. http://dx.doi.org/10.1016/0040-5809(90)90002-D.

Urban, M.C., Bocedi, G., Hendry, A.P., Crozier, L.G., Meester, L. De, Godsoe, W., Gonzalez, A., Hellmann, J.J., Holt, R.D., Huth, A., Johst, K., Krug, C.B., Leadley, P.W., Palmer, S.C.F., Pantel, J.H., Schmitz, A., Zollner, P.A., Travis, J.M.J, 2016. Improving the forecast for biodiversity under climate change. Science 353 (6304).

Walters, R.J., Berger, D., 2019. Implications of existing local (mal)adaptations for ecological forecasting under environmental change. Evol. Appl. (ISSN: 1752-4571, 1752-4571) 12 (7), 1487–1502. http://dx.doi.org/10.1111/eva.12840.

Waxman, D., Peck, J.R., 1999. Sex and adaptation in a changing environment. Genetics (ISSN: 1943-2631) 153 (2), 1041–1053. http://dx.doi.org/10.1093/genetics/153.2.1041.